



Chromosomal translocation t(11;14) and p53 deletion induced by the CRISPR/Cas9 system in normal B cell-derived iPS cells

メタデータ	言語: English 出版者: 公開日: 2022-05-24 キーワード (Ja): キーワード (En): 作成者: 阿左見, 祐介 メールアドレス: 所属:
URL	https://fmu.repo.nii.ac.jp/records/2000391

学 位 論 文

Chromosomal translocation $t(11;14)$ and $p53$
deletion induced by the CRISPR/Cas9 system
in normal B cell-derived iPS cells

(B 細胞由来 iPS 細胞における CRISPR/Cas9 システム
を用いた $t(11;14)$ 染色体転座と $p53$ 遺伝子欠失)

福島県立医科大学大学院医学研究科

腫瘍内科学分野 腫瘍内科学講座

阿左見 祐介

Chromosomal translocation $t(11;14)$ and *p53* deletion induced by the CRISPR/Cas9 system in normal B cell-derived iPS cells

Author: Yusuke Azami, Department of Medical Oncology, Fukushima Med. Univ. School of Medicine, Fukushima, 960-1295, Japan

Figures: 4

Supplemental Figures: 10

Funding:

This work was supported in part by a Grant-in-Aid for Scientific Research (C), No. 20K08738 and by a Grant-in-Aid for Young Scientists, No. 20K16795, from the Japanese Ministry of Education, Culture, Sports, Science, and Technology, The Japanese Society of Hematology Research Grant, Japan Leukemia Research Fund, and Network-type Joint Usage/Research Center for Radiation Disaster Medical Science.

Disclosure of Potential Conflicts of Interest:

The authors declare that they have no conflict of interests.

論 文 内 容 要 旨

しめい 氏名	あざみ ゆうすけ 阿左見 祐介
学位論文題名	Chromosomal translocation t(11;14) and <i>p53</i> deletion induced by the CRISPR/Cas9 system in normal B cell-derived iPS cells (B 細胞由来 iPS 細胞における CRISPR/Cas9 システムを用いた t(11;14) 染色体転座と <i>p53</i> 遺伝子欠失)
<p>【背景】 多発性骨髄腫 (Multiple Myeloma: MM) 細胞は, Immunoglobulin heavy chain (<i>IgH</i>) の解析から成熟 B 細胞由来とされる. MM の発症は <i>IgH</i> のある 14 番染色体と <i>CCND1</i> (Cyclin D1) のある 11 番染色体などとの相互転座が原因となることが多い. 骨髄腫細胞起源は成熟 B 細胞 (または形質細胞) が再プログラミングされた状態で染色体異常 (転座) や遺伝子異常が起こった細胞との仮説をたてた. そこで正常 B 細胞から iPS 細胞 (B cell-derived Induced Pluripotent Stem Cells: BiPSCs) を樹立し, DNA2 本鎖切断に関与する activation-induced cytidine deaminase (AID) を tet-off システムで発現誘導できる正常 B 細胞由来 iPS 細胞を樹立した (BiPSC13-AID, MIB2-6-AID) (Sci Rep, 2017). 今回, この BiPSCs に CRISPR/Cas9 system を用いて染色体転座 (cTr) t(11;14) を誘導し, さらに MM の増悪に関与する遺伝子変異である <i>p53</i> 欠失を生じさせ, この細胞が造血前駆細胞 (HPC), さらに B 細胞へ分化誘導可能か検討することで MM の起源細胞を再現できるのではないかと考えた.</p> <p>【方法】 2 種類の BiPSCs に CRISPR/Cas9 システムを用い染色体転座 t(11;14) を誘導し, さらに, BiPSC13-AID with t(11;14) において <i>p53</i> を欠失させた. HPC の分化は, STEMdiff™ Hematopoietic Kit (KIT 分化法) を使用した. B 細胞系への分化誘導法は, マウスストローマ細胞 (MS-5) との共培養法を行った.</p> <p>【結果】 染色体転座 t(11;14) を持つ BiPSC13-AID を作製し (AX-AID), さらに <i>p53</i> 欠失したものを G#28-AID とした. これら BiPSCs (BiPSC13-AID, AX-AID, G#28-AID) は, KIT 分化法にて CD34 陽性細胞が得られた. この CD34 陽性細胞は細胞表面抗原解析から CD38-/CD43+/CD45+ であり, colony forming assay にて顆粒球, マクロファージ, 赤芽球を含むコロニー形成が確認でき HPC と考えられた. また, B 細胞系への分化誘導実験では, 臍帯血由来の CD34 陽性細胞では CD10-/CD19+ の細胞集団の出現が確認できたが, AX-AID または G#28-AID 由来の CD34 陽性細胞ではリンパ球様細胞への分化誘導はみられなかった.</p> <p>【結論】 BiPSCs に CRISPR/Cas9 システムを用いて多発性骨髄腫発生を模倣すると考えられる遺伝子変異をおこした. これらゲノム編集した BiPSCs は HPC へ分化誘導可能であった. しかし, 臍帯血とは異なり, BiPSCs から分化誘導した HPC は, MS-5 共培養法では B 細胞系への分化誘導は認められなかった.</p>	

※日本語で記載すること。1200字以内にまとめること。

CONTENTS

LIST OF ABBREVIATIONS.....	2
ABSTRACT.....	3
INTRODUCTION.....	4
MATERIALS AND MERHODS.....	6
RESULTS.....	14
DISCUSSION.....	20
REFERENCES.....	24
FIGURE LEGENDS.....	27
FIGURES.....	34

LIST OF ABBREVIATIONS

MM: Multiple myeloma

IgH: immunoglobulin heavy chain

cTr: chromosomal translocation

CCND1: cyclin D1

BiPSCs: B cell-derived induced pluripotent stem cells

HPCs: hematopoietic progenitor cells

BM: bone marrow

AID: activation-induced cytidine deaminase

CRISPR: clustered regularly interspaced short palindromic repeats

sgRNA: single guide RNA

CB: cord blood

PAM: protospacer adjacent motif

CSR: class switch recombination

SHM: somatic hypermutations

FL: follicular lymphoma

MCL: mantle cell lymphoma

ABSTRACT

Multiple myeloma (MM) cells are derived from mature B cells based on immunoglobulin heavy chain (*IgH*) gene analysis. The onset of MM is often caused by a reciprocal chromosomal translocation (cTr) between chr 14 with *IgH* and chr 11 with Cyclin D1 (*CCND1*). We propose that mature B cells gain potential to transform by reprogramming, and then chromosomal aberrations cause the development of abnormal B cells as a myeloma-initiating cell during B cell redifferentiation. To study myeloma-initiating cells, we have already established normal B cell-derived induced pluripotent stem cells (BiPSCs). Here we established two BiPSCs with reciprocal cTr t(11;14) using the CRISPR/Cas9 system; the cleavage sites were located in the *IgHE μ* region of either the VDJ rearranged allele or non-rearranged allele of *IgH* and the 5' -upstream region of the *CCND1* (two types of BiPSC13 with t(11;14) and MIB2-6 with t(11;14)). Furthermore, *p53* was deleted using the CRISPR/Cas9 system in BiPSC13 with t(11;14). These BiPSCs differentiated into hematopoietic progenitor cells (HPCs). However, unlike cord blood, those HPCs did not differentiate into B lymphocytes by co-culture with BM stromal cell. Therefore, further ingenuity is required to differentiate those BiPSCs-derived HPCs into B lymphocytes.

INTRODUCTION

The cellular origin of multiple myeloma (MM) has not been identified. Based on the experiments of transplantation of bone marrow (BM) samples from MM patients into immunodeficient mice, so-called myeloma stem cells have been inferred to be present in CD19⁻/CD38⁺⁺/CD138⁺ or CD138⁻ plasma cell populations^{1,2}; however, the results may indicate the presence of plasma cell populations with cell proliferation ability rather than the cellular origin of myeloma cells. On the other hand, based on immunoglobulin heavy chain (*IgH*) gene analysis, myeloma cells are derived from post germinal center B cells³ (Figure S1). Chromosomal aberrations such as trisomy and chromosomal translocation (cTr) play a critical role in early tumorigenesis of MM^{4,5}. We established induced pluripotent stem (iPS) cells from normal B lymphocytes (BiPSCs: BiPSC13 and MIB2-6) to test the hypothesis that the abnormal cells of origin responsible for tumorigenesis of MM are reprogrammed mature B lymphocytes⁶, and these BiPSCs have the same VDJ rearrangement of *IgH* as the original B lymphocytes and differentiate into CD34⁺/CD38⁻ hematopoietic progenitor cells (HPCs) when co-cultured with stromal cells. Furthermore, these cells can induce the expression of activation-induced cytidine deaminase (AID) that causes mutations not only in *IgH* but also in other genes, and further causes double strand breaks in DNA.

Here we generated BiPSCs with reciprocal cTr t(11;14), which is reciprocal translocation between *IgH* and *CCND1* and the most frequent cTr in MM^{4,5}, using the clustered regularly interspaced short palindromic repeats (CRISPR)/Cas9 system⁷. Furthermore, we generated BiPSC13 with t(11;14) with a deletion in exon 5 of *p53* because deletion of *p53* is involved in the progression of MM^{4,5} (Figure S2). Subsequently, we analyzed the

features of cTr t(11;14) between the functional allele or the non-functional allele of *IgH* and *CCND1* and the ability to differentiate into blood cells.

If we can induce the chromosomal translocations and genetic abnormalities seen in MM in the established iPS cell lines and differentiate them into hematopoietic progenitor cells and then into B cells, they will serve as model cells to support our hypothesis.

We assessed differentiation potential of established iPS cell lines (BiPSCs, BiPSCs with reciprocal cTr t(11;14), BiPSCs with t(11;14) and a deletion *p53*) into HPC, and B lymphocyte.

MATERIALS AND MERHODS

Materials

Plasmids used in this study, lentiCRISPRv2 (#98290) were obtained from Addgene (www.addgene.org). lentiCRISPRv2 was a gift from Brett Stringer. Synthetic oligonucleotides and PCR primers were purchased from Eurofin Genomics (Tokyo, Japan). DNAiso was purchased from Takara bio (Kyoto, Japan). Thunderbird® SYBR qPCR Mix and KOD-FX Neo were obtained from Toyobo (Tokyo, Japan). PEI_{max} 40000 was obtained from Polyscience Inc. (Warrington, PA, USA).

Normal B cell-derived iPS cell (BiPSCs: BiPSC13, MIB2-6) culture

Established BiPSCs were maintained in a six-well plate coated with iMatrix-511 (Nippi, Tokyo, Japan) in BiPSC culture medium, StemFit® AK02N (REPROCELL, Yokohama, Japan). The BiPSC culture medium was changed every day until the start of differentiation experiment using the STEMdiff Hematopoietic Kit (STEMCELL Technologies, Vancouver, Canada).

Induction of translocation

cTr was induced by infection of BiPSCs with *IgH-CCND1* lentiCRISPRv2 lentivirus which targets the human *IgH* E μ region and 13kb upstream of the *CCND1* coding sequence (CDS)⁷. Briefly, CRISPRscan (<http://www.crisprscan.org/>)⁸ estimated the gRNA candidate, 5'-GGAGAACATACCAAGCCCCAC-3' for *IgH* (105,861,064 to 105,861,045 of NC_000014.9, chromosome (chr) 14, GRCh38.p12 Primary Assembly)

and 5'-GGTGGCGAGGTGGGACCGCGG-3' for *CCND1* (69,627,757 to 69,627,776 of NC_000011, chr 11, GRCh38.p12 Primary Assembly), which were recombined into the lentiCRISPRv2 BsmBI site. The *CCND1* gRNA expression unit of *CCND1*-lentiCRISPRv2 was cloned into *IgH*-lentiCRISPRv2 to form the *IgH-CCND1* lentiCRISPRv2 dual site targeting vector. The vector was packaged into lentivirus, and BiPSCs cultures were infected with the packaged virus in the presence of polybrene (4 µg/mL) for 1 day. Puromycin selection (0.25 µg/mL) started after 2 days. Ten days later, drug-resistant colonies were picked and mechanically divided into two portions using pipet tips; one half was cultured, and DNA was isolated from the other half using DNAiso kit. Confirmation of cTr was performed by PCR using the *IgH/CCND1* translocation-specific primer pair (*IgH*-Fs for the *IgH* side and *CCND1*-86-Rs for the *CCND1* side) (Figure 1, Table S1) with Thunderbird® SYBR qPCR Mix and a Light Cycler Nano (Roche Diagnostics, Basel, Switzerland). PCR conditions were 94° C 120 sec, 50 cycles of (94° C 10 sec, 62° C 10 sec, 72° C 20 sec), and 72° C to 94° C at 0.1° C /sec for melting temperature measurement. The presence of Tr-positive clones was assessed based on the melting temperature of PCR-amplified DNA compared with positive control DNA, which was the product amplified from the *IgH* and *CCND1* genomic region with PCR and recombined into a translocation-mimic PCR template (5'-*IgH-CCND1*-3')⁷.

Detection of VDJ and DJ rearrangements in BiPSCs

Confirmation of the VDJ recombination profile was performed as described⁹. Briefly, VDJ regions from BiPSC genomic DNA were amplified with PCR using primer pairs of VHn-FR1 (n = 1-6) and JH consensus for the functional *IgH* allele, and DH regions were amplified using primer pairs of DHn (n = 1-7) and JH consensus for the non-functional

IgH allele. Primers are listed in Table S1. PCR conditions are 95° C 120 sec, 45 cycles of (95° C 30 sec, 62° C 15 sec, 72° C 40 sec) using TB Green® Fast qPCR Mix and LightCycler Nano. PCR products were electrophoresed in an agarose gel, and bands of the corresponding size were purified using FastGene Gel/PCR Extraction Kit (NIPPON Genetics) and sequenced with the same primers for PCR (FASMAC Co. Ltd.). Sequence data were analyzed using the IgBLAST database (<https://www.ncbi.nlm.nih.gov/igblast/>) to identify the subtype of every subdomain. An additional primer, DH5-18-F was used for DNA sequence of the non-functional *IgH* allele of MIB2-6.

Identification of reciprocal chromosomal translocation t(11;14)

VH3-FR1 primer for BiPSC13 or VH4-FR1 primer for MIB2-6 was used in combination with the CCND1-86-F primer to detect reciprocal cTr, which formed der(11)t(11;14), between the functional *IgH* allele and CCND1. DH2 primer for BiPSC13 or DH5 primer for MIB2-6 was used with the CCND1-86-F to detect reciprocal cTr, which formed der(11)t(11;14) between the non-functional *IgH* allele and CCND1. The combination of IgH-Fs and CCND1-86-R or CCND1-86-Rs was used to detect another reciprocal cTr forming der(14)t(11;14). The presence of the untranslocated allele of *IgH* was confirmed with PCR in the combinations of DH2 or VH3-FR1 and IgH-Fs for BiPSC13 and DH5 or VH4-FR1 and IgH-Fs for MIB2-6, respectively. The presence of the untranslocated allele of *CCND1* was confirmed with PCR in the combination of CCND1-86-F and CCND1-86-R for both BiPSCs (Figure 1A-F). Long PCR was performed using KOD FX Neo DNA polymerase and LifeTouch (BIOER Tech., Hangzhou, P. R. China). PCR conditions were 94° C 120 sec, 35 cycles of (94° C 10 sec, 64° C 10 sec, 68° C 3 min). PCR products were electrophoresed in agarose gels, and gel images were obtained in a

ChemDoc XRS+ Imaging System and Image Lab 4.1 software (BIO-RAD, Hercules, CA, USA). Exposure time to obtain images was automatically adjusted to detect faint bands by the software. For DNA sequencing, major bands were purified using FastGene Gel/PCR Extraction Kit (Nippon Genetics, Tokyo, Japan).

DNA sequences were analyzed by FASMAC (Atsugi, Japan) using primers for PCR positioned at translocation junction sites. Obtained sequences were aligned to *IgH* or *CCND1* genome sequences to confirm sequence identity and alterations using ApE (<http://jorgensen.biology.utah.edu/wayned/ape/>) and NCBI Blast (<https://blast.ncbi.nlm.nih.gov/>). The existence of the non-translocated allele of *IgH* was also confirmed with PCR in the combination of VH3-FR1 primer for BiPSC13 or VH4-FR1 primer for MIB2-6 with IgH-Fs in the same condition of long PCR for the detection of cTr described above. All primers are listed in Table S1.

TP53 knockout using the CRISPR/Cas9 system

The CRISPR/Cas9 system was used to disrupt expression of *TP53*¹⁰. The pSpCas9(BB)-2A-GFP (PX458) vector was a gift from Feng Zhang (Addgene plasmids # 48138). In brief, a single guide RNA (sgRNA) sequence was selected using E-CRISP (<http://www.e-crisp.org/E-CRISP/index.html>). The sgRNA sequence for *TP53* Exon 5 was 5'-GTTGATTCCACACCCCGCC, which corresponds to the sequence on the 3' side of the initiation codon of $\Delta 133p53$. The plasmid expressing hCas9 and *TP53* sgRNA was prepared by ligating oligonucleotides into the BbsI site of PX458 (TP53ex5/PX458). To generate a *TP53* knockout clone, 1 μ g TP53ex5/PX458 plasmid was nucleofected into BiPSC13 with t(11;14) (AX) (1×10^6 cells) using a 4D-Nucleofector™ instrument (Lonza Japan, Tokyo, Japan). After 3 days, cells expressing GFP were sorted using

FACSAria (BD Bioscience, Franklin Lakes, NJ, USA), and single-cell cloning was performed. A single clone was selected, expanded, and used for biological assays. For sequence analysis of *TP53* exon 5, the following primer set was used to amplify genomic DNA: 5'-TTGCAGGAGGTGCTTACACA and 5'-GAATTCTGAAGGTCTCGTCGT.

Culture of BiPSCs in stem cell differentiation medium for differentiation into HPCs

Differentiation of BiPSCs into HPC was performed using STEMdiff™ Hematopoietic Kit (STEMCELL Technologies, Vancouver, Canada). BiPSCs were cultured on Matrigel® hESC-Qualified Matrix (Corning, NY, USA), incubated with Gentle Cell Dissociation Reagent (STEMCELL Technologies) at room temperature for 4-6 min, removed using a scraper, and then, 50 μ m-sized pieces were transferred to a matrigel-coated 12-well plate in Complete StemFit® AK02N (100 pieces/well). Differentiation experiments were performed according to the instructions of the kit. BiPSCs with AID were cultured in the presence of 10 ng/mL doxycycline (Takara Bio, Kusatsu, Japan) to prevent AID expression. Concurrently, CD34⁺ cells were purified using MACS CD34 MicroBeads (Miltenyi Biotec Inc., Auburn, CA, USA) according to the manufacturer's instructions, and the collected cells were used for phenotype analysis and a colony-forming assay.

Phenotype analysis

Purified CD34⁺ cells were evaluated by two-color and three-color flow cytometry after staining in phosphate-buffered saline without calcium chloride or magnesium chloride with the following monoclonal antibodies: anti-CD19-PE, anti-CD34-PE (BioLegend, San Diego, CA, USA), anti-CD38-FITC, anti-CD43-FITC, anti-CD10-FITC (BioLegend),

and anti-CD45-PE/Cy5 (BioLegend). Immunofluorescence of the labeled cell membrane was evaluated using a flow cytometer (S3e™ Cell Sorter; BIO-RAD). Furthermore, phenotype analysis was performed after co-culture of CD34⁺ cells with MS-5¹¹.

Colony-forming assay

Purified CD34⁺ cells were then used in colony-forming assays using Methocult H4435 (STEMCELL Technologies) in triplicate. The types of colonies formed were assessed around day 14.

cTr t(11;14)-specific fluorescence in situ hybridization (FISH)

cTr t(11;14)-specific FISH was performed by LSI Medience (LSI Medience Corporation, Tokyo, Japan).

Western blot analysis

The method was described in our previous study⁶. Briefly, cells were lysed in lysis buffer (0.5% NP-40, 1% TritonX-100, 150 mM NaCl, and 1 mM EDTA in 20 mM Tris, pH 7.5) with a protease inhibitor cocktail (Nacalai Tesque, Kyoto, Japan) and PhosSTOP phosphatase inhibitor cocktail (Roche Diagnosis). After ten min on ice, the cell lysates were centrifuged at 14,000 rpm for 10 min at 4° C and the supernatants were recovered. Protein content of every sample was measured by Bradford method, and protein of 70 µg aliquots were separated in a Mini-PROTEAN TGX precast Gel (BIO-RAD) and transferred to a nitrocellulose membrane (BIO-RAD). The membrane was incubated with the indicated antibodies and horseradish peroxidase (HRP)-labeled secondary

antibodies, and the signal was visualized with enhanced Chemi-Lumi One Super (Nacalai Tesque) and detected by the ChemDoc XRS+ (BIO-RAD). The primary antibodies used were anti-AICDA (Abcam Japan, Tokyo, Japan), p53 (DO-1) (Santa Cruz Biotech, Dallas, TX, USA), and anti-GAPDH (Abcam) and the second antibody was goat anti-mouse IgG-HRP or goat anti-rabbit IgG-HRP (Santa Cruz Biotech).

Co-culture of purified CD34⁺ cells or cord blood (CB) with MS-5 for differentiation into B lymphocyte

The murine BM stromal cell line MS-5¹¹ (a kind gift from Dr. Katsuhiko Itoh, Kyoto University), was maintained in α -MEM (Nacalai Tesque) supplemented with 20% horse serum (HS) (JRH (SAFC) Biosciences, Inc. Lenexa, KS, USA) and 1% penicillin/streptomycin (PS) (Nacalai Tesque). The cells were cultured to approximately 80% confluency in a FALCON tissue culture flask 50mL (CORNING) for co-culture with purified CD34⁺ cells differentiated from BiPSC13, MIB2-6 and G#28-AID, or in a six-well tissue plate (Becton Dickinson, Franklin Lakes, NJ, USA) for co-culture with human CD34⁺ progenitor cells from cord blood (CB) (hCD34⁺-CB, single donor; Takara Bio). CD34⁺ cells (1×10^4 cells/mL) derived from BiPSC13, MIB2-6 and G#28-AID, and 0.5×10^4 cells/mL of CD34⁺ cells from CB, were plated onto the MS-5 feeder cells in α -MEM supplemented with 10% FBS, 1% GlutaMAXTM (Thermo Fisher Scientific KK, Tokyo, Japan), 1-thioglycerol (4×10^{-4} M, Sigma-Aldrich Japan, Tokyo, Japan), SCF (50 ng/mL) (BioLegend), G-CSF (25 ng/mL) (BioLegend), Flt3-L (50 ng/mL) (BioLegend), and IL-7 (20 ng/mL) (BioLegend). All cultures were performed in a humidified incubator containing 5% CO₂ in air at 37° C. Every 7 days, the cells were fed by removing half of the medium and replacing it with fresh medium containing fresh

cytokines. Samples of CB co-cultured with MS-5 were collected after 10 days, 4 weeks and 6 weeks of co-culture, and the other samples were collected after 3-5 weeks of co-culture. For phenotype analysis, co-culture supernatant was collected, the MS-5 layer was incubated with collagenase IV (1 mg/mL) for 20 min at 37° C, then the supernatant and MS-5 were combined and subjected to phenotype analysis.

RESULTS

Construction of IgH/cyclin D1-specific CRISPR/Cas9

The *CCND1* cleavage site on chr 11 was upstream of *CCND1* where off-target effects are fewer and setting a protospacer adjacent motif (PAM) site is easy, based on a study showing no hot spots at the cleavage site in the analysis of MM patients¹². The *IgH* cleavage site on chr 14 was targeted at a site with fewer off-target effects, between E μ and I μ in the class switch region of *IgH*, and where setting a PAM site is easy¹³. We then designed a CRISPR/Cas9 vector in which these were arranged in tandem to obtain artificial induction of t(11;14) by cutting *CCND1* upstream on chr 11 and between E μ and I μ regions of *IgH* on chr 14. We designed two efficient gRNA sequences to be expressed in one CRISPR/Cas9 vector⁷. The functioning of this system was confirmed by induction of cTr t(11;14) in 293T cells⁷. We attempted to induce reciprocal cTr t(11;14) in two normal B lymphocyte-derived iPS cell lines (BiPSC13, MIB2-6) using the above method. In both BiPSC13 and MIB2-6, *IgH* has a complete VDJ rearrangement (VH3-FR1: V₃₋₉D₄₋₂₃J₂ in BiPSC13, VH4-FR1: V₄₋₃₉D₃₋₂₂J₆ in MIB2-6), no class switch recombination (CSR) of *IgH* (Figure S3), and no somatic hypermutations (SHM) in the VDJ region compared to germline (Figure S4A and S4C).

Two pairs of *IgH* on chr 14 and *CCND1* on chr 11 of BiPSC13 and MIB2-6 are shown in Figure 1A and 1D. In BiPSC13, the upper and lower alleles of chr 14 show the non-functional allele that stopped at DJ rearrangement (D₂₋₂₁J₂) and the functional allele that completed VDJ rearrangement (V₃₋₉D₄₋₂₃J₂) of *IgH*, respectively (Figure S4A and S4B). In MIB2-6, the upper and lower alleles of chr 14 show the non-functional allele in which DJ rearrangement was incomplete (D₅₋₁₈J₄), and the functional allele in which VDJ

rearrangement was complete ($V_{4-39}D_{3-22}J_6$) for *IgH*, respectively (Figure S4C and S4D). The DJ joining of the non-functional allele of MIB2-6 was incomplete because DH4, DH6, and DH7 were deleted between D_{5-18} and J_4 , but an intron of 1000 bases or more remained (Figure S4D).

Using the CRISPR/Cas9 system, we induced two kinds of reciprocal cTr t(11;14), in which the translocation allele of *IgH* was different, in BiPSC13 and MIB2-6 (BiPSC13 t(11;14) and MIB2-6 t(11;14), respectively). AZ and AX were the different types of BiPSC13 t(11;14) carrying either the VDJ-rearranged allele or the DJ-rearranged allele of *IgH*, respectively, that reciprocally translocated with *CCND1* (Figure 1B and 1C). BC and BG were the different types of MIB2-6 t(11;14) carrying either the VDJ-rearranged allele or the DJ-rearranged allele of *IgH*, respectively, that reciprocally translocated with *CCND1* (Figure 1E and 1F).

The features of these cTrs were confirmed with PCR using translocation-specific primers (Figure 1). The PCR product in lane 1 shows the presence of the VDJ-rearranged functional allele of *IgH*, and the PCR product in lane 2 shows the non-functional allele that stopped at DJ rearrangement of *IgH*. Therefore, the PCR product in lane 3 shows the translocation between the functional allele of *IgH* and *CCND1*, and the PCR product in lane 4 shows the translocation between the non-functional allele of *IgH* and *CCND1* (Figure 1G and 1H). Among these cTrs, when the VDJ side of the *IgH* functional allele translocated with *CCND1* upstream, der(11)t(11;14) was formed. Simultaneously, the CDS side of *CCND1* translocated with the constant region of *IgH*, and der(14)t(11;14) was formed (AZ and BC) (Figure 1B, 1E, and 1G-I). On the other hand, when the DJ side of the non-functional allele of *IgH* translocated with *CCND1* upstream, der(11)t(11;14) was formed. Simultaneously, the CDS side of *CCND1* translocated with

the constant region of *IgH*, and der(14)t(11;14) was formed (AX and BG) (Figure 1C, 1F, and 1G-I). Therefore, we established cell lines carrying reciprocal cTr t(11;14) between *CCND1* and either an allele in which VDJ rearrangement of *IgH* was completed or an allele in which VDJ rearrangement was not completed (stopped at DJ joining) in BiPSC13 t(11;14) (AZ and AX) and MIB2-6 t(11;14) (BC and BG), respectively. We also confirmed the reciprocal cTr t(11;14) using IGH-*CCND1* FISH (Figure 1J and 1K). Subsequently, we analyzed the nucleotide sequences near the translocation sites of AZ and AX, and BC and BG (Figure 1L and 1M). Thirteen-base deletion of the *CCND1* gRNA region and three-base deletion of the *IgH* gRNA region in der(11)t(11;14) of AX, and three-base addition at the translocation junction in der(14)t(11;14) of AX were confirmed (Figure 1L). The cleavage site was 140 bases downstream from the PAM region of *CCND1* gRNA in der(11)t(11;14) of BC, and 11-base deletion in the *CCND1* gRNA region was confirmed (Figure 1M). One-base deletion in the *CCND1* gRNA and 30-base deletion in the E μ direction from the *IgH* gRNA in der(11)t(11;14) of BG, and 2-base deletion in the *IgH* gRNA region in der(14)t(11;14) of BG were confirmed (Figure 1M).

Effects of CRISPR/Cas9 on alleles of *IgH* not used in the translocation with *CCND1* and on alleles of *CCND1* not used in the translocation with *IgH* were also analyzed (Supplemental information, Figure S5 and S6). Deletions from 11 bases to 333 bases were found around the cleavage sites of Cas9 in those BiPSCs.

Knockout of TP53 with the CRISPR/Cas9 system

Because deletion of chr 17p, including *p53* deletion, is involved in the progression of MM, genome editing was performed on *p53* in BiPSC13 t(11;14) (AX) using the

CRISPR/Cas9 system. The expression of TP53 was knocked out by deleting 83 bp of exon 5 of *p53* (G#28: Figure 2). Subsequently, we established G#28 and AX with AID expression regulated by the doxycycline-controlled (Tet-off) system (G#28-AID and AX-AID)⁶ (Figure S7).

Summary of BiPSCs

BiPSC13 is iPS cell line from human B lymphocyte in BM.

MIB 2-6 is iPS cell line from human B lymphocyte in peripheral blood.

AZ is BiPSC13 t(11;14) of the *IgH* functional allele.

AX is BiPSC13 t(11;14) of the *IgH* non-functional allele.

BC is MIB2-6 t(11;14) of the *IgH* functional allele.

BG is MIB2-6 t(11;14) of the *IgH* non-functional allele.

G#28-AID is AX with *TP53* knock out and AID expression regulated by the doxycycline-controlled (Tet-off) system.

Differentiation of BiPSCs into blood cells

Initially, the induction of differentiation into HPC was performed by co-culturing BiPSC13, MIB2-6 with AGM-S3¹⁴ (Figure S8). However, the differentiation efficiency was not stable, and AGM-S3 contamination was present even after purification using CD34 microbeads. We then used the STEMdiff™ Hematopoietic Kit to induce differentiation of BiPSCs into HPCs (Figure 3). Based on a model of hematopoietic differentiation from human embryonic stem cells¹⁵, the expression of CD43, CD45, and CD38 was examined in CD34⁺ cells. Except for AX (Figure 3C), two cell populations were

observed (R1 and R2), and most CD34⁺ cells were CD43⁺/CD45⁺/CD38^{+/-} in both populations (Figure 3). The number of colonies formed in the colony assay is shown in Figure 3I. Most colonies were a mix of macrophages and granulocytes, and some were mixed with erythroblasts (Figure 3A-3D, 3G, and 3H). BC differentiated into CD34⁺ cells, but colony formation was not observed (Figure 3F). On the other hand, differentiation into blood cells was observed even in the case of *p53* deletion and induction of AID expression in the colony assay in AX (Figure 3G and 3H). Therefore, B cell-derived iPS cells were able to differentiate into HPCs even in the presence of cTr t(11;14) or *p53* deletion.

Differentiation of BiPSCs-derived CD34⁺ cells and cord blood (CB) into B lymphocyte

We investigated whether HPCs differentiated from iPS cells derived from normal B lymphocytes can differentiate into B lymphocyte again by co-culture with MS-5, with reference to a study by MacLean¹⁶. First, we confirmed that CB would differentiate into B lymphocytes by co-culture with MS-5, with reference to studies by Nishihara¹⁷ and Hirose¹⁸. CB proliferated rapidly after initiating the co-culture, and phenotype analysis at day 10 revealed that CD34⁺ cells were mainly present in the R2 region (Figure 4A). The main cell population in both the R1 and R2 regions was CD34⁻/CD38^{+/-}/CD43⁺/CD45⁺, followed by CD34⁺/CD38⁻/CD43⁺/CD45⁺ (Figure 4A). Four weeks after initiating the co-culture, the CD34⁺ cells had disappeared and the main cell populations were CD34⁻/CD38^{+/-}/CD43⁺/CD45⁺, and CD19⁺/CD10⁻ cells were observed in R2 region (Figure 4B). The number of CD19⁺/CD10⁻ cells further increased 6 weeks after initiation of the co-culture (Figure 4B).

Next, we investigated whether two types of BiPSCs (BiPSC13 and MIB2-6) would differentiate into B lymphocytes by co-culture with MS-5. The cells were differentiated into CD34⁺ cells using a STEMdiff™ Hematopoietic kit, and purified CD34⁺ cells were subsequently cultured on MS-5. Phenotype analysis was performed 3 weeks after initiation of the co-culture, with reference to a previous study¹⁶. Based on studies reporting the appearance of CD19⁺ cells from the fourth week of co-culture of CB with MS-5^{17,18}, we performed phenotype analyses 4 or 5 weeks after initiation of the co-culture. Analysis of BiPSC13-derived cells showed a non-specific cell population, even after staining with an isotype control using FITC or without staining (Figure S9). Therefore, the cell population observed by the double staining of CD34/CD38 and CD19/CD10 was likely to be due to autofluorescence. In the co-culture of BiPSC13 or MIB2-6-derived CD34⁺ cells with MS-5, the CD34⁺ cells remained mainly in the R1 region, and their phenotype were CD34⁺/CD38⁻/CD43⁻/CD45⁻ (Figure 4C and 4D). A population of CD34⁻/CD38⁻/CD43⁺/CD45⁺ cells was also observed (Figure 4C and 4D). No CD19⁺ cells were observed. In the co-culture of G#28-AID-derived CD34⁺ cells with MS-5, CD34⁺ cells were still found in both the R1 and R2 regions and their phenotype was CD34⁺/CD38⁻/CD43⁻/CD45⁻ (Figure 4E).

Therefore, the critical difference between these three types of BiPSCs-derived HPCs and CB was that the former CD34⁺ cells remained and did not differentiate into CD38⁺ cells even after 4 weeks of co-culture with MS-5.

DISCUSSION

We hypothesized that the abnormal cells from which myeloma cells originate may be mature B lymphocytes with chromosomal or genetic changes in the reprogrammed state that enable them to acquire the potential to become tumor cells during the process of redifferentiation into B lymphocytes. Here we tried to generate cells to test this hypothesis. First, we established iPS cells from normal B lymphocytes (BiPSCs) that can induce AID expression⁶. We then generated BiPSCs carrying the most frequent reciprocal cTr t(11;14) in MM (BiPSC13 t(11;14) and MIB2-6 t(11;14)), and also generated BiPSC13 t(11;14) with *p53* deletion, which is involved in the progression of MM. This means “Strike (chromosomal or genetic changes) while the iron (B lymphocytes) is hot”. Studies have reported the possibility of generating reprogrammed tumor cells or precancerous lesions by forcibly expressing the Yamanaka factors in colonic epithelium or pancreatic acinar cells that already have gene mutations^{19,20}. Interestingly, *in vivo* reprogramming is possible in the presence of inflammation and senescence instead of Yamanaka factors, and depolarization of the original cell is considered to be critical²¹. We believe that normal B lymphocytes could be transformed into iPS-like cells in the environment of BM or lymph nodes in which Yamanaka factors are induced due to chronic inflammation. The original cells of BiPSCs were normal cells, unlike the cells mentioned above^{19,20}, and genomic changes were induced after transformation into iPS cells.

The onset of MM is often caused by a reciprocal cTr between chr 14 with *IgH* and chr 11 with *CCND1* or chr 4 with *FGFR3* and *MMSET*^{4,5}. In follicular lymphoma (FL) and mantle cell lymphoma (MCL), immature B lymphocytes in BM are considered the origin of tumor cells; the reciprocal cTr between *IgH* and oncogenes such as *BCL-2* on chr 18

or *CCND1* on chr 11 during VDJ rearrangement is responsible for tumorigenesis of B lymphocytes²². On the other hand, in MM, mature B lymphocytes, so-called plasma cells, or antibody-producing cells, are considered tumor cells because *IgH* reciprocally translocate with other genes during CSR^{23,24}, and SHM is recognized in the VDJ region of *IgH*⁵⁻²⁷. Considering the presence of M-protein, a functional allele of *IgH* is present in MM. Therefore, cTr occurs between another non-functional allele of *IgH* in which VDJ rearrangement has not been completed, and other chromosomes in MM³. The features of cTr in AX and BG exactly mimic that of MM.

When VDJ rearrangement of one allele of *IgH* is complete, VDJ rearrangement of another allele of *IgH* is not complete as a non-functional allele due to allelic exclusion^{28,29}. In FL and MCL, cTr occurs during VDJ rearrangement in immature B lymphocytes as mentioned above. However, considering that B-cell receptors are expressed on the cell surface, the allele that initiates VDJ rearrangement earlier would be a non-functional allele due to cTr, and in turn, another allele that should have been non-functional, would undergo VDJ rearrangement to create a functional allele that expresses B-cell receptors. Although cTr during VDJ rearrangement in MM was also reported³⁰, many cTrs occur during CSR^{4,5}.

Even in immature B lymphocytes, cTr t(14;18) or cTr t(11;14) alone is believed to not be able to transform these B lymphocytes, as suggested by studies revealing these chromosomal aberrations in normal individuals³¹⁻³³. Similarly, mature B lymphocytes would be unlikely to transform into tumor cells by cTr. Myeloma cells could be derived from reprogrammed mature B lymphocytes with the following features: the CD19 antigen on the cell surface and its transcription factor, Pax5, are deleted in myeloma cells unlike in other B cell lymphomas³⁴. Furthermore, myeloma cells expressing CD33³⁵, which is a

cell surface marker of granulocytes, or producing amylase^{36,37} or ammonia³⁸ have been reported.

Myeloma cells are derived from mature B lymphocytes because of SHM in the VDJ region of *IgH* (Figure S10). Because neither SHM in the VDJ region nor CSR of *IgH* occurred in BiPSC13 or MIB2-6, those BiPSCs are considered to be derived from pre-germinal center (GC) B lymphocytes rather than mature B lymphocytes. However, they can induce AID expression with the tet-off system⁶, and we confirmed that those BiPSCs and BiPSCs with t(11;14) can differentiate into HPCs in this study. If they further redifferentiate into B lymphocytes, SHM in the VDJ region and CSR of the functional allele of *IgH* could be induced during the redifferentiation process by activation of endogenous AID. Furthermore, activation of enhancers involved in *IgH* expression during the process of redifferentiation into B lymphocytes would lead to overexpression of *CCND1* induced by cTr t(11;14), which is observed in MM with t(11;14). Expression of AID also would be expected to induce SHMs on various genes other than *IgH*, which would lead to the branching pathway theory based on a Darwinian selection perspective³⁹, a model for the progression of MM. In addition, if *IgH* expression is impossible due to a deletion in the constant region instead of CSR in the functional allele, this would be considered a mechanism of development of Bence-Jones-type MM; only the light chain of the M-protein is detected in the urine (and serum), because myeloma cells in these cases do not produce the IgH chain.

Unfortunately, no CD19⁺ cells were observed in co-culture of BiPSCs-derived CD34⁺ cells with MS-5. The difference between these BiPSCs-derived HPCs and CB was that the former CD34⁺ cells remained and CD34⁻/CD43⁺/CD45⁺ cells did not express CD38 even after 4 weeks of co-culture with MS-5. Especially, compared with the parent cell

(BiPSC13), G#28-AID did not differentiate into CD34⁻/CD43⁺/CD45⁺ cells with remaining of CD34⁺ cells even 6 weeks after the initiation of co-culture with MS-5. A deletion of *p53* might be involved in this feature. Given that CD38 is involved in lymphocyte activation^{40,41}, the ability to express CD38 in differentiation from HPC could be important for differentiation into B lymphocytes. Considering the results of the colony assay, a differentiation potential into blood cells of BiPSCs-derived HPCs can be expected, so other factors could be required for co-culture with MS5 in order to differentiate them into B lymphocytes in vitro. We considered that BiPSCs-derived HPCs is inferior to CB in terms of differentiation potential into B lymphocytes. We presume that the unsuccessful to induce B lymphocyte may be due to a problem in the process of differentiation from BiPSCs to CD34 positive cells. There are possibilities that some of the CD34 positive cells may be HPC, but the percentage is small or CD34 positive cells have differentiation directivity into myeloid lineage. We need to search a way to amplify and purify HPCs in more undifferentiated state. And we are planning to compare the single cell RNA analysis during the differentiation process to that of CB to see how important transcription factors are expressed. This information may give us a key to induce HPCs in a state like CB. Moreover, important questions are whether these BiPSCs with *cTr* or *p53* deletion are capable of forming MM or B lymphoid tumor cells, and whether AID induction induces additional genetic aberrations. We are planning to transplant these BiPSC-derived HPCs into BM of immunodeficient mice.

REFERENCES

1. Hosen, N. *et al.* CD138-negative clonogenic cells are plasma cells but not B cells in some multiple myeloma patients. *Leukemia* **26**, 2135–2141 (2012).
2. Kim, D., Park, C. Y., Medeiros, B. C. & Weissman, I. L. CD19- CD45low/- CD38high/CD138+ plasma cells enrich for human tumorigenic myeloma cells. *Leukemia* **26**, 2530–2537 (2012).
3. González, D. *et al.* Immunoglobulin gene rearrangements and the pathogenesis of multiple myeloma. *Blood* **110**, 3112–3121 (2007).
4. Morgan, G. J., Walker, B. A. & Davies, F. E. The genetic architecture of multiple myeloma. *Nat. Rev. Cancer* **12**, 335–348 (2012).
5. Kumar, S. K. *et al.* Multiple myeloma. *Nat. Rev. Dis. Prim.* **3**, 1–20 (2017).
6. Kawamura, F. *et al.* Establishment of induced pluripotent stem cells from normal B cells and inducing AID expression in their differentiation into hematopoietic progenitor cells. *Sci. Rep.* **7**, 1–11 (2017).
7. Tsuyama, N. *et al.* Induction of t(11;14) igh enhancer/promoter-cyclin d1 gene translocation using crispr/cas9. *Oncol. Lett.* **18**, 275–282 (2019).
8. Doench, J. G. *et al.* Optimized sgRNA design to maximize activity and minimize off-target effects of CRISPR-Cas9. *Nat. Biotechnol.* **34**, 184–191 (2016).
9. van Dongen, J. J. M. *et al.* Design and standardization of PCR primers and protocols for detection of clonal immunoglobulin and T-cell receptor gene recombinations in suspect lymphoproliferations: Report of the BIOMED-2 concerted action BMH4-CT98-3936. *Leukemia* **17**, 2257–2317 (2003).
10. Ota, A. *et al.* Δ40P53A Suppresses Tumor Cell Proliferation and Induces Cellular Senescence in Hepatocellular Carcinoma Cells. *J. Cell Sci.* **130**, 614–625 (2017).
11. Itoh, K. *et al.* A novel hematopoietic multilineage clone, Myl-D-7, is stromal cell-dependent and supported by an alternative mechanism(s) independent of stem cell factor/c-kit interaction. *Blood* **87**, 3218–3228 (1996).
12. Ronchetti, D. *et al.* Molecular analysis of 11q13 breakpoints in multiple myeloma. *Blood* **93**, 1330–1337 (1999).
13. Fenton, J. A. L., Pratt, G., Rothwell, D. G., Rawstron, A. C. & Morgan, G. J. Translocation t(11;14) in Multiple Myeloma: Analysis of Translocation Breakpoints on der(11) and der(14) Chromosomes Suggests Complex Molecular Mechanisms of Recombination. *Genes Chromosom. Cancer* **39**, 151–155 (2004).
14. Xu, M. J. *et al.* Stimulation of mouse and human primitive hematopoiesis by murine embryonic aorta-gonad-mesonephros-derived stromal cell lines. *Blood* **92**, 2032–

- 2040 (1998).
15. Vodyanik, M. A., Thomson, J. A. & Slukvin, I. I. Leukosialin (CD43) defines hematopoietic progenitors in human embryonic stem cell differentiation cultures. *Blood* **108**, 2095–2105 (2006).
 16. MacLean, G. A. *et al.* Downregulation of Endothelin Receptor B Contributes to Defective B Cell Lymphopoiesis in Trisomy 21 Pluripotent Stem Cells. *Sci. Rep.* **8**, 1–10 (2018).
 17. Nishihara, M. *et al.* A combination of stem cell factor and granulocyte colony-stimulating factor enhances the growth of human progenitor B cells supported by murine stromal cell line MS-5. *Eur. J. Immunol.* **28**, 855–864 (1998).
 18. Hirose, Y. *et al.* B-cell precursors differentiated from cord blood CD34+ cells are more immature than those derived from granulocyte colony-stimulating factor-mobilized peripheral blood CD34+ cells. *Immunology* **104**, 410–417 (2001).
 19. Hashimoto, K. *et al.* Cellular context-dependent consequences of Apc mutations on gene regulation and cellular behavior. *Proc. Natl. Acad. Sci. U. S. A.* **114**, 758–763 (2017).
 20. Shibata, H. *et al.* In vivo reprogramming drives Kras-induced cancer development. *Nat. Commun.* **9**, 1–7 (2018).
 21. Taguchi, J. & Yamada, Y. Unveiling the Role of Senescence-Induced Cellular Plasticity. *Cell Stem Cell* **20**, 293–294 (2017).
 22. Lieber, M. R. Mechanisms of human lymphoid chromosomal translocations. *Nat. Rev. Cancer* **16**, 387–398 (2016).
 23. Bergsagel, P. L. *et al.* Cyclin D dysregulation: An early and unifying pathogenic event in multiple myeloma. *Blood* **106**, 296–303 (2005).
 24. Chesi, M. *et al.* AID-Dependent Activation of a MYC Transgene Induces Multiple Myeloma in a Conditional Mouse Model of Post-Germinal Center Malignancies. *Cancer Cell* **13**, 167–180 (2008).
 25. Vescio, R. A. *et al.* Myeloma Ig heavy chain V region sequences reveal prior antigenic selection and marked somatic mutation but no intraclonal diversity. *J. Immunol.* **155**, 2487–97 (1995).
 26. Sahota, B. S. S. *et al.* Myeloma VL and VH gene sequences reveal a complementary imprint of antigen selection in tumor cells. *Blood* **89**, 219–226 (1997).
 27. Kosmas, C. *et al.* Origin and diversification of the clonogenic cell in multiple myeloma: Lessons from the immunoglobulin repertoire. *Leukemia* **14**, 1718–1726 (2000).
 28. Chang, Y., Bosma, M. J. & Bosma, G. C. Extended duration of DH-JH rearrangement

- in immunoglobulin heavy chain transgenic mice: Implications for regulation of allelic exclusion. *J. Exp. Med.* **189**, 1295–1305 (1999).
29. Jung, D., Giallourakis, C., Mostoslavsky, R. & Alt, F. W. Mechanism and control of V(D)J recombination at the immunoglobulin heavy chain locus. *Annu. Rev. Immunol.* 541–570 (2006).
 30. Morgan, G. *et al.* Characterization of IgH breakpoints in multiple myeloma indicates a subset of translocations appear to occur in pre-germinal center B cells. *Blood* **121**, 3413–3420 (2013).
 31. Yasukawa, M. *et al.* Low frequency of BCL-2/JH translocation in peripheral blood lymphocytes of healthy Japanese individuals. *Blood* **98**, 486–488 (2001).
 32. Roulland, S. *et al.* Follicular lymphoma-like B cells in healthy individuals: A novel intermediate step in early lymphomagenesis. *J. Exp. Med.* **203**, 2425–2431 (2006).
 33. Lecluse, Y. *et al.* T(11;14)-Positive Clones Can Persist Over a Long Period of Time in the Peripheral Blood of Healthy Individuals. *Leukemia* **23**, 1190–1193 (2009).
 34. Mahmoud, M. S. *et al.* Altered expression of Pax-5 gene in human myeloma cells. *Blood* **87**, 4311–4315 (1996).
 35. Matsuo, Y. *et al.* Establishment and characterization of new IgD lambda type myeloma cell lines, MOLP-2 and MOLP-3, expressing CD28, CD33 antigens and the IL-6 receptor. *Human cell* **6**, 310–313(1993).
 36. Matsuzaki, H., Hata, H., Takeya, M. & Takatsuki, K. Establishment and characterization of an amylase-producing human myeloma cell line. *Blood* **72**, 978–982 (1988).
 37. Ohtsuki, T. *et al.* Two human myeloma cell lines, amylase-producing KMS-12-PE and amylase-non-producing KMS-12-BM, were established from a patient, having the same chromosome marker, t(11;14)(q13;q32). *Br. J. Haematol.* **73**, 199–204(1989).
 38. Matsuzaki, H. *et al.* Human Myeloma Cell Line (KHM-4) Established from a Patient with Multiple Myeloma Associated with Hyperammonemia. *Intern. Med.* **31**, 339–343 (1992).
 39. Anderson, K. *et al.* Genetic variegation of clonal architecture and propagating cells in leukaemia. *Nature* **469**, 356–361 (2011).
 40. Schneider, M. *et al.* CD38 is expressed on inflammatory cells of the intestine and promotes intestinal inflammation. *PLoS One* **10**, 1–16 (2015).
 41. Glaría, E. & Valledor, A. F. Roles of CD38 in the Immune Response to Infection. *Cells* **9**, 228 (2020).

FIGURE LEGENDS

Figure 1. Features of the reciprocal chromosomal translocation (cTr) between *CCND1* on chr 11 and *IgH* on chr 14

(A) (D) Two pairs of *IgH* on chr 14 and *CCND1* on chr 11 of BiPSC13 and MIB2-6 are shown. The cleavage site of CRISPR/Cas9 is indicated by (\uparrow). The bent arrows and arrowheads indicate the direction of transcription of *CCND1* and *IgH*, respectively. CCND1-86F, CCND1-86R, IgH-Fs, DH2, DH5, VH3-FR1, VH4-FR1, IgHu-LoF represent PCR primers for the confirmation of cTr t(11;14). (B) Reciprocal cTr between the functional allele ($V_{3-9}D_{4-23}J_2$) of *IgH* and *CCND1* in BiPSC13 (AZ). (E) Reciprocal cTr between the functional allele ($V_{4-39}D_{3-22}J_6$) of *IgH* and *CCND1* in MIB2-6 (BC). (C) Reciprocal cTr between the non-functional allele ($D_{2-21}J_2$) of *IgH* and *CCND1* in BiPSC13 (AX). (F) Reciprocal cTr between the functional allele ($D_{5-18}J_4$) of *IgH* and *CCND1* in MIB2-6 (BG). (G)(H) Confirmation of reciprocal cTr between *IgH* and *CCND1* with PCR. PCR in BiPSC13 and two types of BiPSC13 with t(11;14) (AZ and AX) (G) and PCR in MIB2-6 and two types of MIB2-6 with t(11;14) (BC and BG) (H). Refer to (A) and (D) above for the location of each primer. The numbers indicate the length of the PCR product estimated from the database. (I) Confirmation of der(14)t(11;14) and der(11)t(t(11;14)) in AZ, AX, BC, and BG with PCR. Refer to (A) and (D) above for the location of each primer. (J) (K) Chromosomal t(11;14)-specific FISH of AZ and AX (J), and BC and BG (K). One chr 11 and chr 14 was reciprocally translocated. *CCND1* and *IgH* probes are labeled with red and green boxes, respectively. The arrowheads indicate the *IgH-CCND1* fusion signal. (L) (M) Reciprocal cTr t(11;14) junction sequence of AZ and AX (L), and BC and BG (M). The dotted line indicates the cleavage site (usually

three bases from the PAM region). Details are described in the results.

Figure 2. Knockout of *p53* with the CRISPR/Cas9 system.

(A) Induction of 83 bp deletion in exon 5 of *p53* using the CRISPR/Cas9 system.

(B) Confirmation of suppression of *p53* expression in G#28 with western blotting.

Induction of apoptosis by H₂O₂ enhanced TP53 expression in wt (BiPSC13), but TP53 expression was not observed in G#28 regardless of H₂O₂ treatment.

Figure 3. Induction of differentiation of parent BiPSCs and their genome edited BiPSCs into blood cells.

(A) BiPSC13, (B) MIB2-6, (C) AX, (D) BG, (E) AZ, (F) BC, (G) AX with AID, and (H) G#28 with AID. (a) Flow cytometric analysis of the cell phenotype after differentiation of BiPSCs into HPCs. Two cell populations were observed (R1 and R2). (b) Representative morphology of formed colonies ($\times 50$). (c) Wright staining of cytopins picked up from a colony ($\times 400$). The bottom picture of (A) and arrows indicate erythroblasts. The bottom picture of (D) shows a mix of macrophages and erythroblasts. (I) Number of colonies formed. The types of colonies formed were assessed in triplicate.

Figure 4. Induction of differentiation into B lymphocytes by co-culture with MS-5.

(A) Ten days after starting co-culture of cord blood (CB) and MS-5. The photo reveals a growth of CB on MS-5. Phenotype analysis of non-adherent floating cells harvested after gentle agitation. CD34⁺ cells are circled with blue dotted lines. Blue arrows, red arrows, and green arrows indicate CD38⁺ cells, CD43⁺ cells, and CD45⁺ cells, respectively. (B) Phenotype analysis of mixed floating and adherent cells 4 and 6 weeks after initiating the

co-culture of CB and MS-5. The cell population indicated by each arrow is the same as in (A). CD19⁺ cells are circled with red dotted lines. (C) Phenotype analysis of mixed floating and adherent cells 3 and 5 weeks after initiating the co-culture of BiPSC13-derived CD34⁺ cells and MS-5. CD34⁺ cells are circled with blue dotted lines. Red arrows and green arrows indicate CD43⁺ cells and CD45⁺ cells, respectively. (D) Phenotype analysis of mixed floating and adherent cells 3 and 4 weeks after initiating the co-culture of MIB2-6-derived CD34⁺ cells and MS-5. The cell populations indicated by blue dotted lines and arrows are the same as in (C). (E) Phenotype analysis of mixed floating and adherent cells 4 and 6 weeks after initiating the co-culture of G#28-AID-derived CD34⁺ cells and MS-5. CD34⁺ cells are circled with blue dotted lines.

Figure S1. B-cell differentiation from pro-B cell to plasma cell and representative cell surface antigens adapted from reference 5.

Pre-B cells express pre-BCR with heavy chain (HC) gene rearrangement. Differentiated B cells and plasma cells from pre-B cells express BCR, which is a complex of an HC and a light chain (LC) with gene rearrangement. BCR, B-cell receptor; SHM, somatic hypermutation.

Figure S2. Hypothesis of the mechanism by which myeloma-initiating cells are born.

If Yamanaka factors would be activated for any reasons in mature B cells, those cells would be reprogrammed to transform to B cell-derived iPS cells (BiPSCs). During the redifferentiation of these BiPSCs into hematopoietic progenitor cells (HPCs) and further into B cells, DNA double-strand breaks (DSBs) would occur in chromosome 14 and another chromosome due to AID expression, resulting in the creation of myeloma-

initiating cells with reciprocal chromosomal translocation (cTr) of these chromosomes. Furthermore, BiPSCs with cTr (t(11;14)) and *p53* deletion differentiate into HPCs, and gene mutations would be induced due to AID expression at the stage of differentiation into B cells, also resulting in the creation of myeloma-initiating cells.

HSC, hematopoietic stem cell; AID, activation-induced cytidine deaminase.

Figure S3. Copy number analysis of the *IgH* constant region.

Each region of the *IgH* constant region ($I\mu$, IgM-Q, IgD-Q, IgG3-Q, and IgG1-Q) was amplified with PCR and compared with that of *CCND1* as a reference to analyze the defect status. Primers are listed in Supplemental Table 1. No decrease in copy number was found in this region in BiPSC13, MIB2-6, and peripheral blood mononuclear cells (PBMNCs), which means that class switch recombination (CSR) has not occurred. The copy numbers of IgM-Q ($C\mu$) and IgD-Q ($C\delta$) were halved in EBV-infected B lymphocyte (C032), which means that CSR has occurred in one allele of *IgH*. No copies were found between IgM-Q and IgG3-Q in KMS-26 (myeloma cell line), which means that CSR to IgG1 has occurred in both alleles of *IgH*.

Figure S4. Nucleotide sequences of both alleles of *IgH* of BiPSC13 and MIB2-6.

(A) The VDJ region of the functional allele of *IgH* of BiPSC13 was consistent with the nucleotide sequence of $V_{3-9}D_{4-23}J_2$, and no somatic mutation was present in that region. N sequences were detected at the junctions between V_{3-9} and D_{4-23} and between D_{4-23} and J_2 .

(B) The non-functional allele of *IgH* of BiPSC13 stopped at DJ rearrangement, and an N sequence was detected at the junction between D_{2-21} and J_2 . (C) The VDJ region of the functional allele of *IgH* of MIB2-6 was consistent with the nucleotide sequence of $V_{4-39}D_3$.

²²J₆, and no somatic mutation was detected in that region. N sequences were detected at the junctions between V₄₋₃₉ and D₃₋₂₂ and between D₃₋₂₂ and J₆. **(D)** The non-functional allele of *IgH* of MIB2-6 was suspected to have ended imperfectly with a gap of more than 1000 bases between D₅₋₁₈ and J₄.

Figure S5. Effects of CRISPR/Cas9 on alleles of *IgH* not used in the translocation with *CCND1*.

(A) The cleavage sites of Cas9 in the vicinity of E μ (between E μ -C μ) of *IgH* of BiPSC13 and MIB2-6 are shown. Both alleles showed no mutation in this region compared with the germline sequence. **(B)** The repair process after cleavage by Cas9 revealed a deletion of 14 bases in the DJ rearrangement allele of AZ, and a deletion of one base in the VDJ rearrangement allele of AX, a deletion of 12 bases in the DJ rearrangement allele of BC and a deletion of 28 bases in the VDJ rearrangement allele of BG.

Figure S6. Effects of CRISPR/Cas9 on alleles of *CCND1* not used in the translocation with *IgH*.

(A) The cleavage sites of Cas9 upstream of the protein-coding sequence of *CCND1* are shown. No mutation was present in this region compared with the germline sequence **(B)**. **(B)** The repair process after cleavage by Cas9 revealed a deletion of 11 bases in AZ, a deletion of 11 bases in AX, a deletion of 11 bases in BG, and a deletion of 333 bases in BC.

Figure S7. qRT-PCR and western blot analysis of AID expression in G#28-AID and AX-AID induced by the doxycycline-controlled (Tet-off) system.

(A) AID expression in G#28-AID and AX-AID in the absence of doxycycline was measured using qRT-PCR. The numbers on the Y axis are the expression of AID mRNA normalized to the expression of GAPDH relative to the expression of AID mRNA of CD19⁺ normal B cells. Data were analyzed in triplicate. (B) AID expression as seen with by western blotting.

Figure S8. Induction of differentiation of BiPSC13 and MIB2-6 into HPCs

Flow cytometric analysis of the cell phenotype after differentiation of BiPSC13 (A) and MIB2-6 (B) into HPCs. CD34⁺ cells were mainly CD43⁻/CD45⁻/CD38⁻.

Figure S9. Phenotype analysis of purified BiPSC13-derived CD34⁺ cells

Purified CD34⁺ cells were evaluated by two-color and three-color flow cytometry after staining with the following antibodies: FITC mouse IgG1, κ isotype Ctrl antibody (BioLegend), PE mouse IgG1, κ isotype Ctrl antibody (BioLegend), and PE/Cyanine5 mouse IgG1, κ isotype Ctrl antibody (BioLegend). Cell populations circled with red dotted lines emitted autofluorescence. Phenotype analysis of mixed floating and adherent cells 3 weeks (A) and 5 weeks (B) after initiating the co-culture of BiPSC13 and MS-5.

Figure S10. Nucleotide sequences of both alleles of *IgH* of two myeloma cell lines, NOP-2⁶ and KMS-12⁷.

(A) Monoclonal VDJ rearrangements of *IgH* (arrows) in NOP-2 detected using PCR. The arrow with # indicates that the height of the peak is less than that of the positive

control in FR3-JH. **(B)** The VDJ region of the functional allele of *IgH* of NOP-2 was consistent with the nucleotide sequence of V₁₋₄₆D₅₋₁₈J₆, and several somatic mutations were present in that region. Red circles indicate amino acid substitutions. N sequences were detected at the junctions between V₁₋₄₆ and D₅₋₁₈ and between D₅₋₁₈ and J₆. **(C)** The non-functional allele of the *IgH* of NOP-2 stopped at DJ rearrangement, and an N sequence was detected at the junction between D₂₋₂₁ and J₅. **(D)** Monoclonal VDJ rearrangements of *IgH* (arrows) in KMS-12 detected using PCR. The arrow with # indicates that the height of the peak is less than that of the positive control in FR2-JH. **(E)** The VDJ region of the functional allele of *IgH* of KMS-12 was consistent with the nucleotide sequence of V₃₋₇D₄₋₂₃J₆, and several somatic mutations were present in that region. Red circles indicate amino acid substitutions. N sequences were detected at the junctions between V₃₋₇ and D₄₋₂₃ and between D₄₋₂₃ and J₆. **(F)** The non-functional allele of *IgH* of KMS-12 stopped at DJ rearrangement, and an N sequence was detected at the junction between D₆₋₂₅ and J₄.

Figure 1

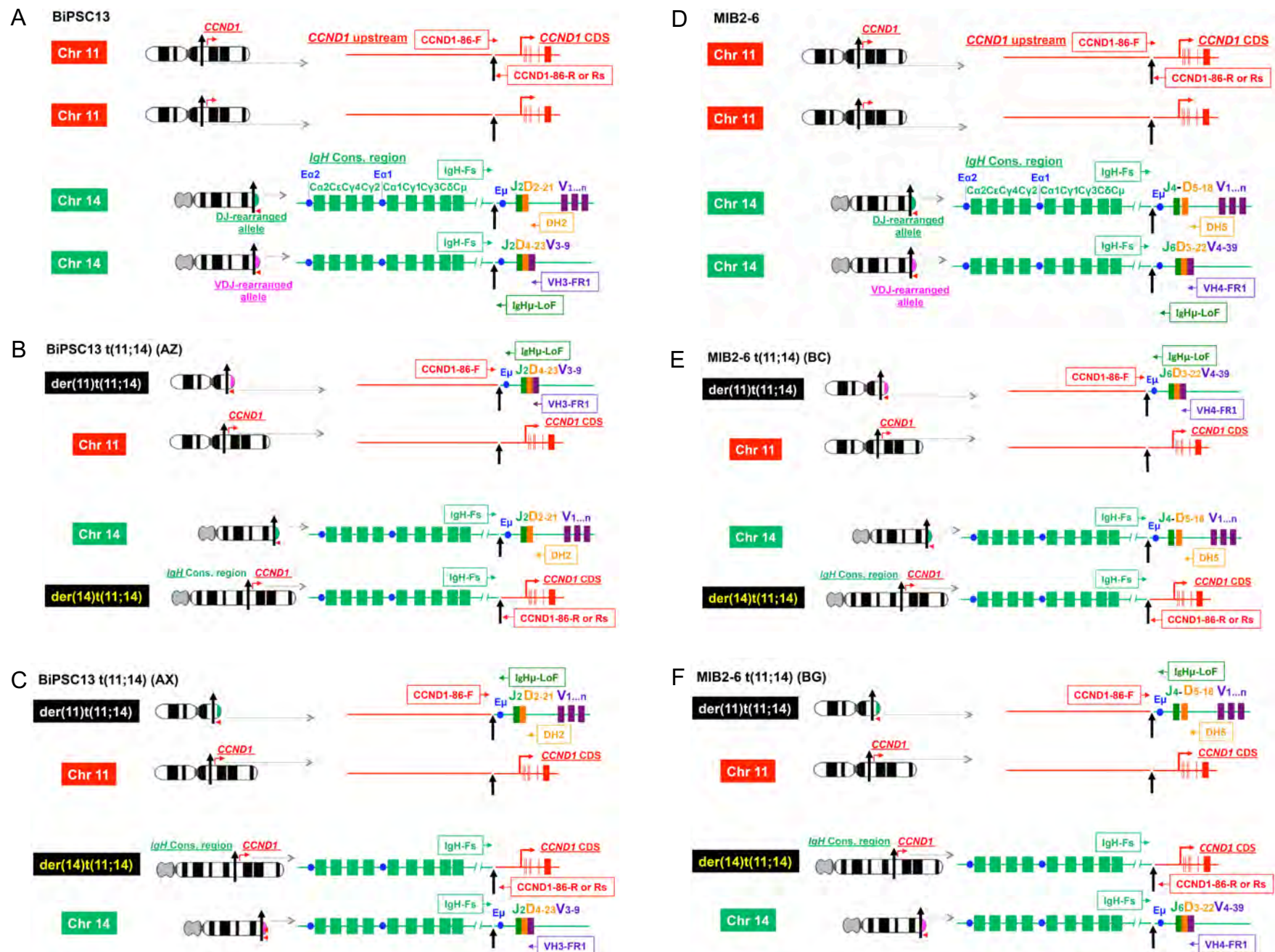
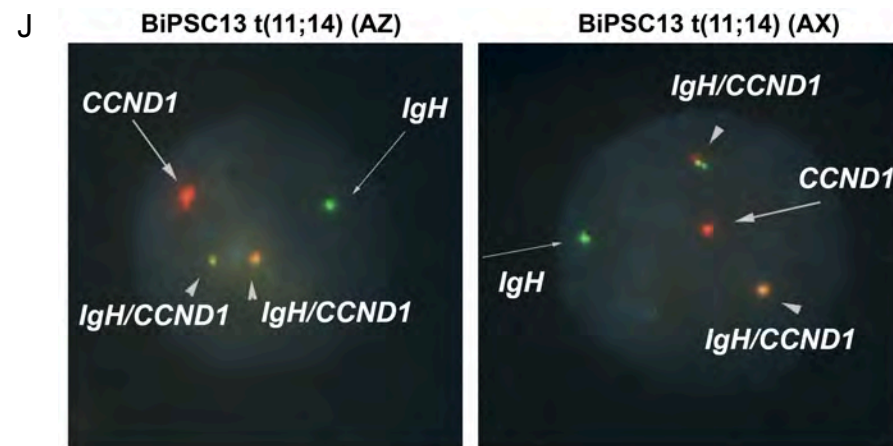
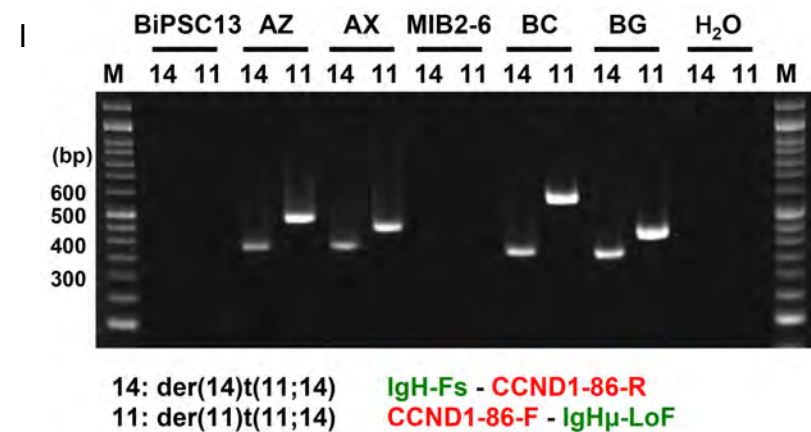
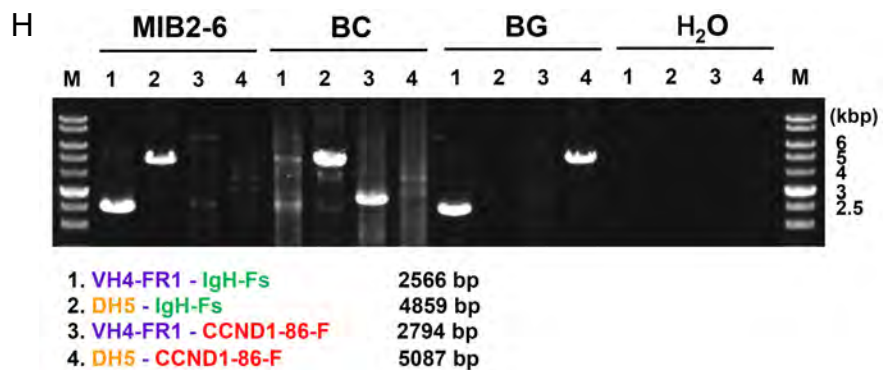
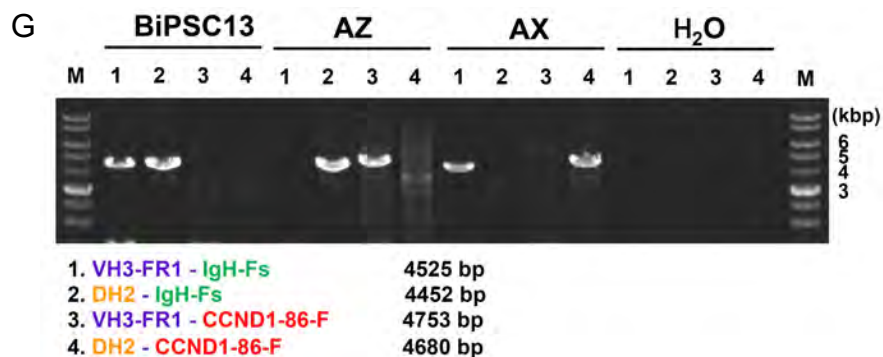
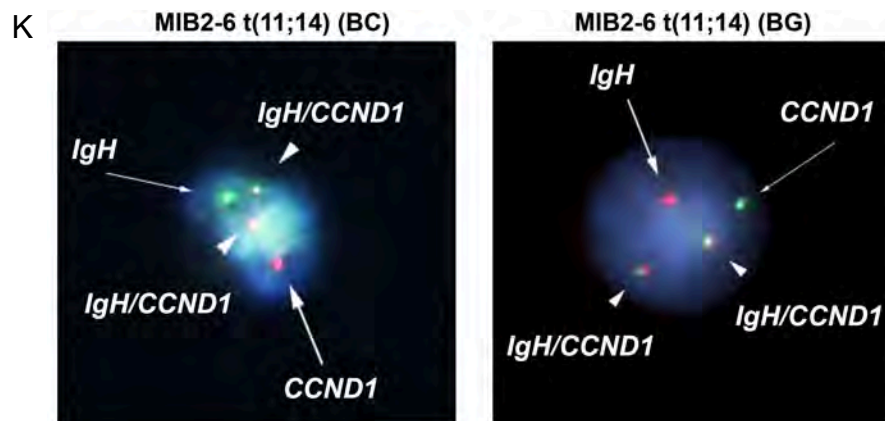


Figure 1



Probe
Green: IgH
Red: CCND1



Probe
Green: IgH
Red: CCND1

Figure 2

A



G#28: 83 bp deletion

WT 5'- CCTGTGCAGCTGTGGGTTGATTCCACACCCCCGCCCGGCACCCGCGTCCGCGCCATGGCCATCT...
 Guide RNA sequence

PAM

TP53^{-/-} 5'- CCTGTGCAGCTGTGGGTTGATTCCACACCCCC---(83 bp deletion)---GCGCTGCC...

B

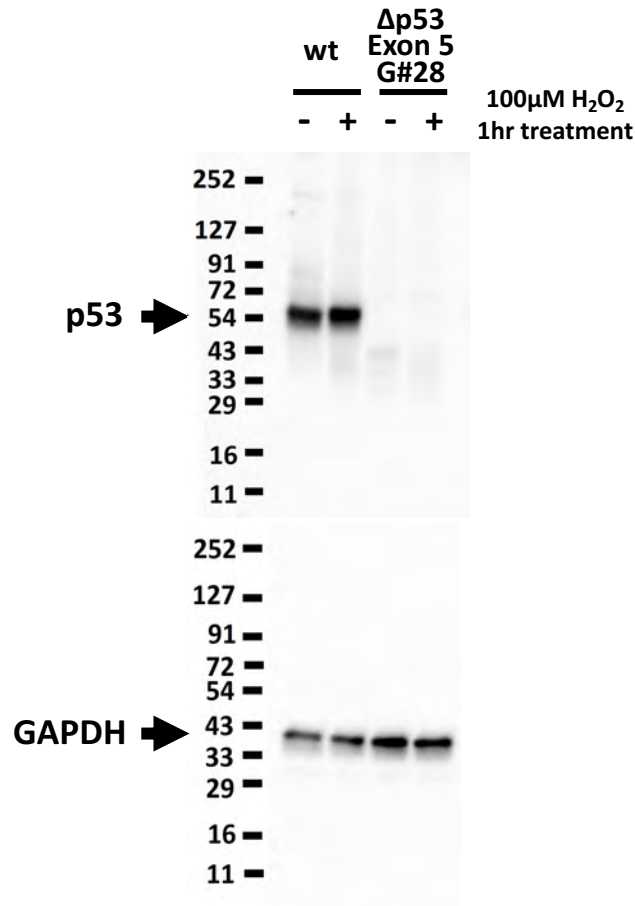


Figure 3

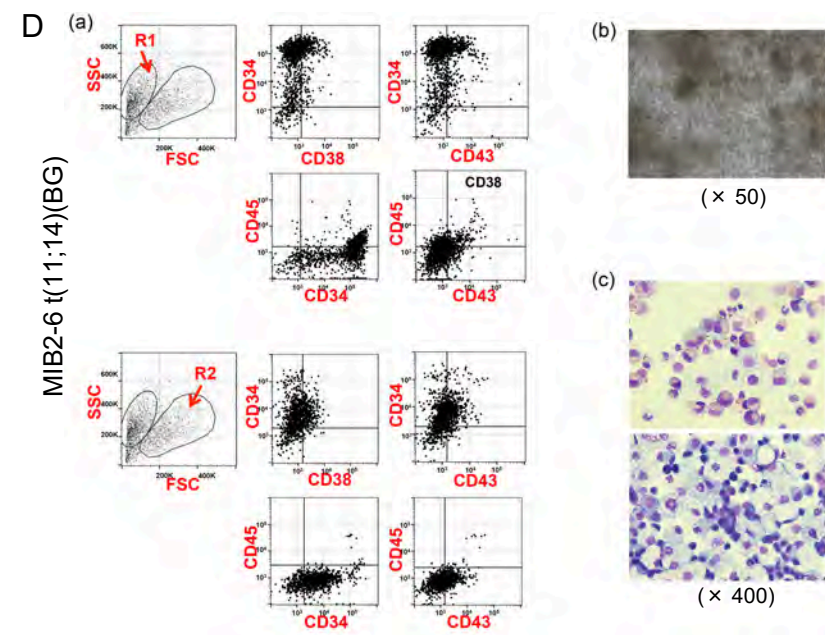
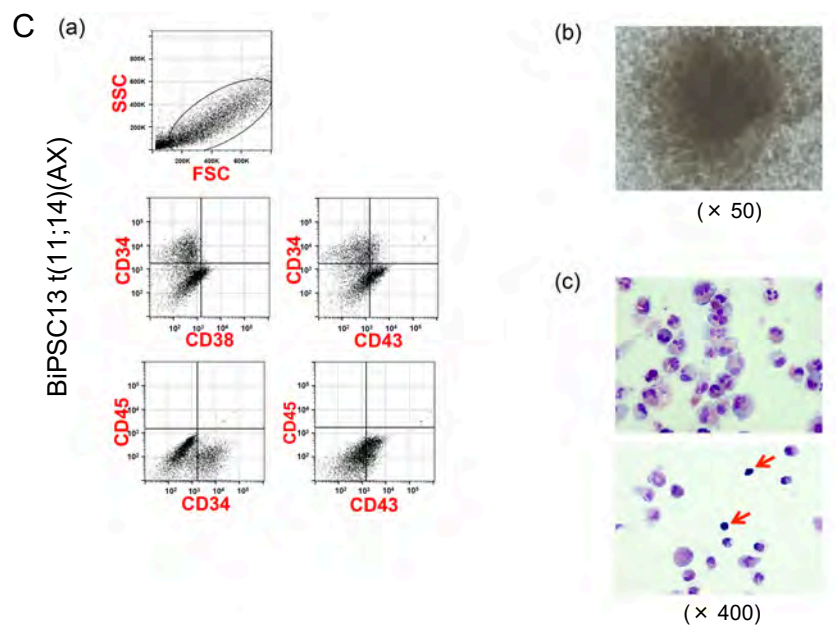
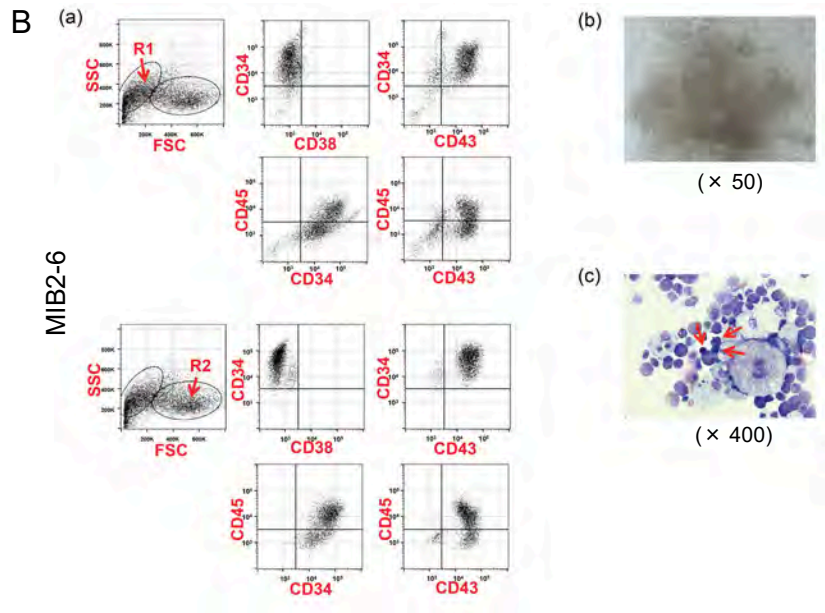
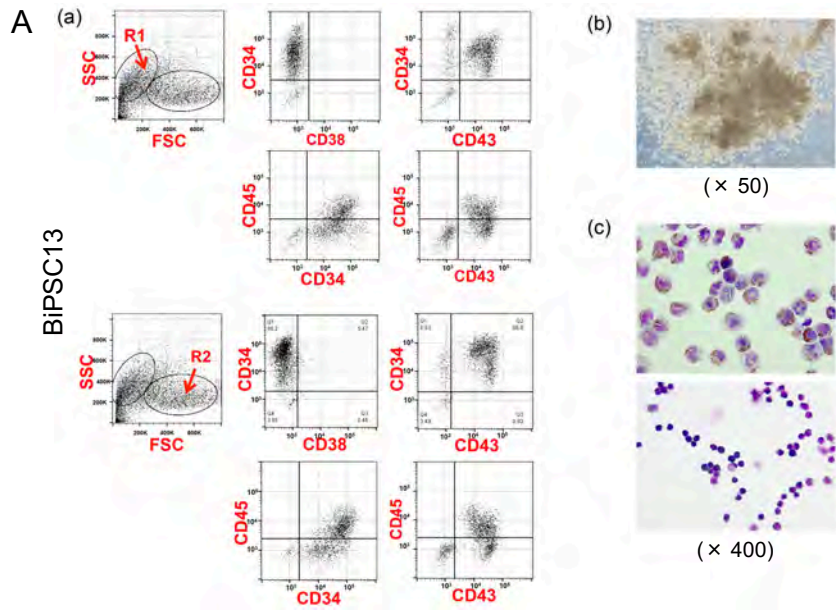
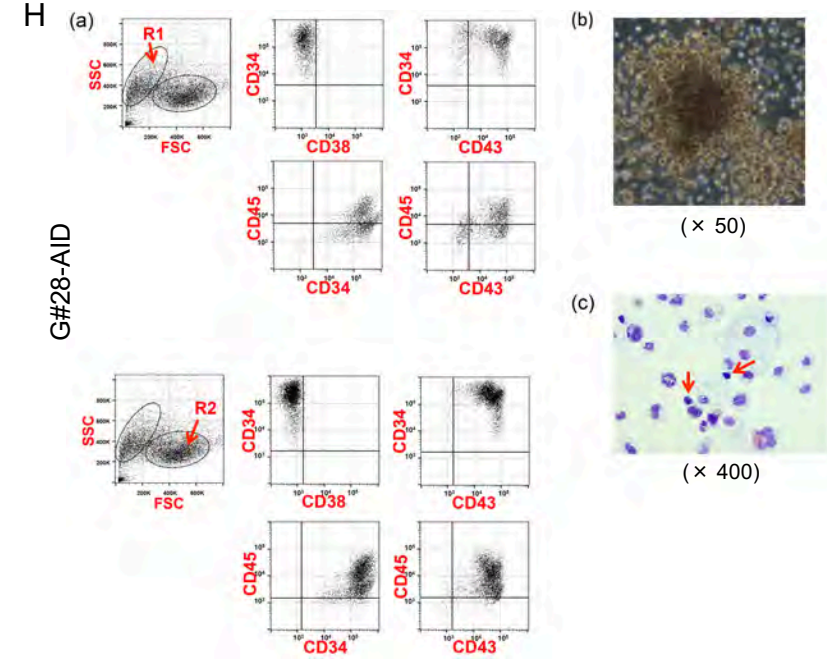
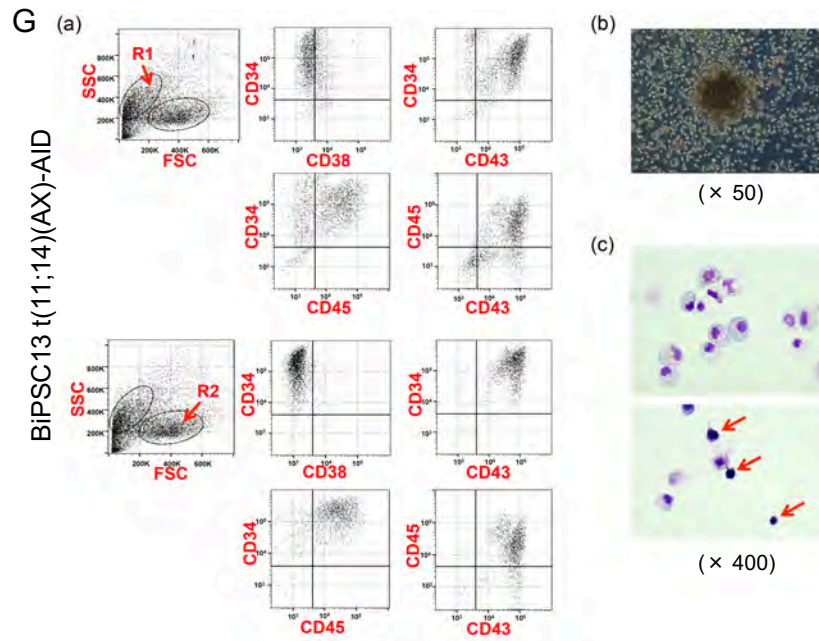
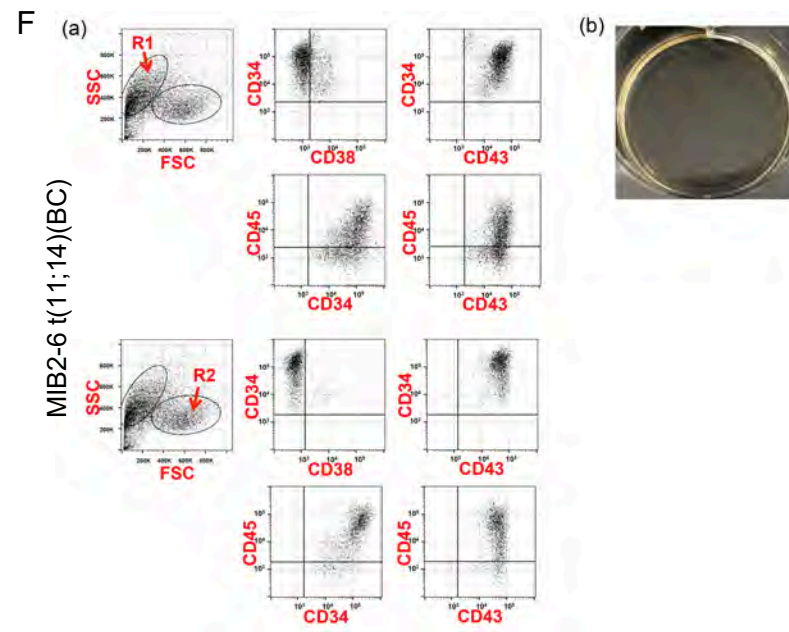
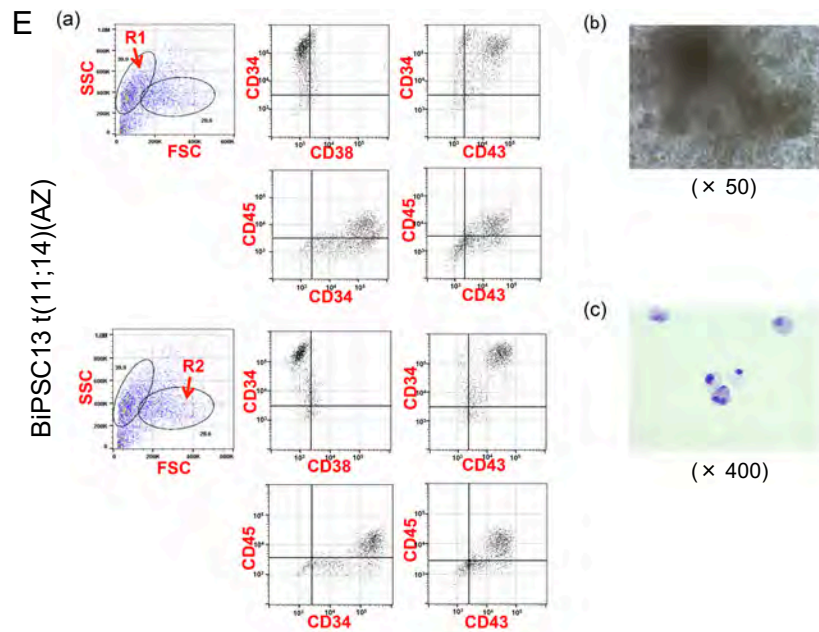


Figure 3



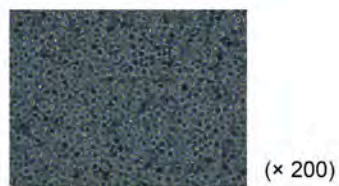
I Number of colonies formed

BiPSCs	Number of colony		
	Well 1	Well 2	Well 3
BiPSC13	12	9	4
MIB2-6	6	6	6
BiPSC13 with t(11;14) (AX)	5	2	3
MIB2-6 with t(11;14) (BG)	3	3	4
BiPSC13 with t(11;14) (AZ)	1	2	3
MIB2-6 with t(11;14) (BC)	0	0	0
BiPSC13 with t(11;14) (AX)-AID	15	18	21
BiPSC13 with t(11;14) p53KD-AID (#28-AID)	10	8	10

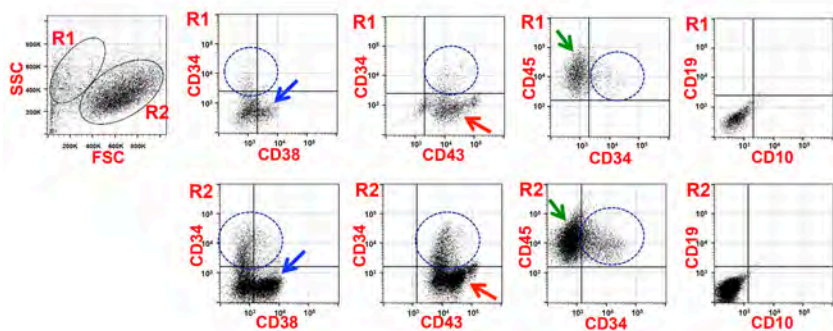
(/3.3 x 10⁴ cells)

Figure 4

A

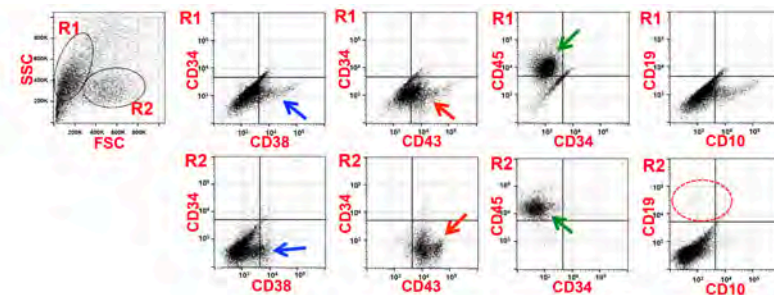


Cord blood/MS-5



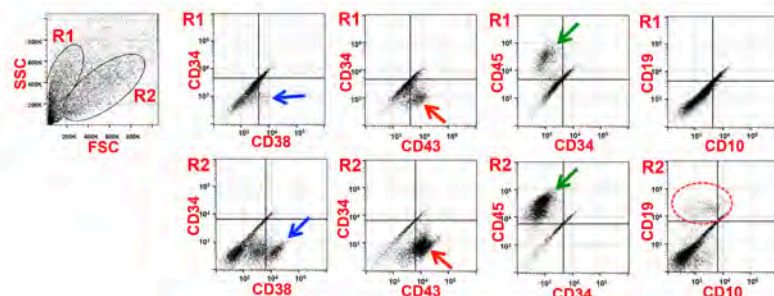
B

4 weeks



Cord blood/MS-5

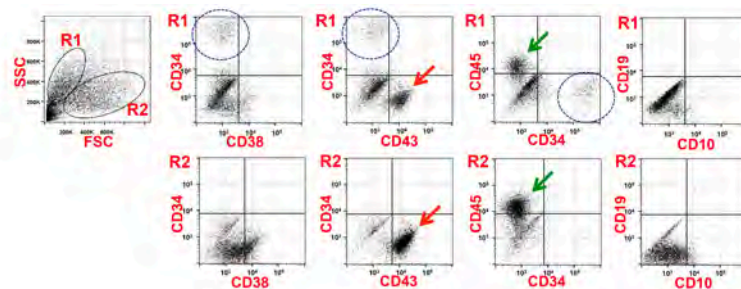
6 weeks



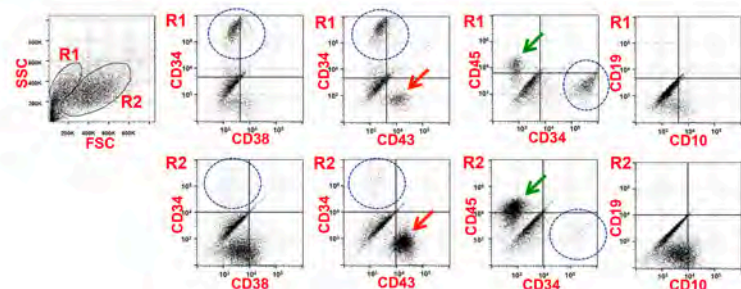
C

BiPSC13-derived CD34⁺ cells/MS-5

3 weeks



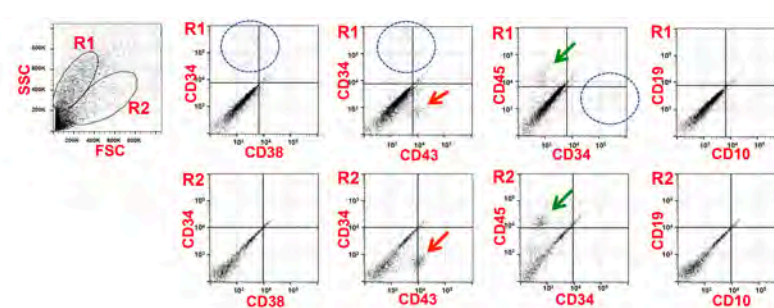
5 weeks



D

MIB2-6-derived CD34⁺ cells/MS-5

3 weeks



4 weeks

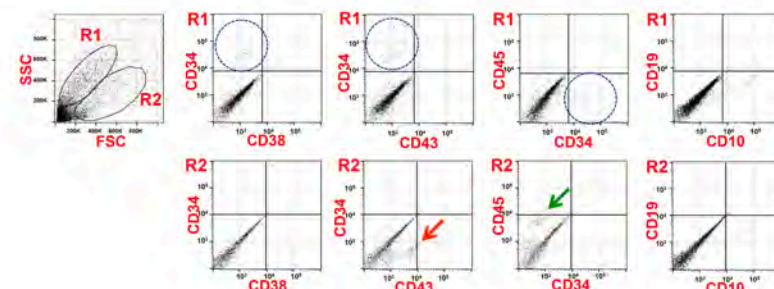


Figure 4

F
G#28-AID-derived CD34⁺ cells/MS-5

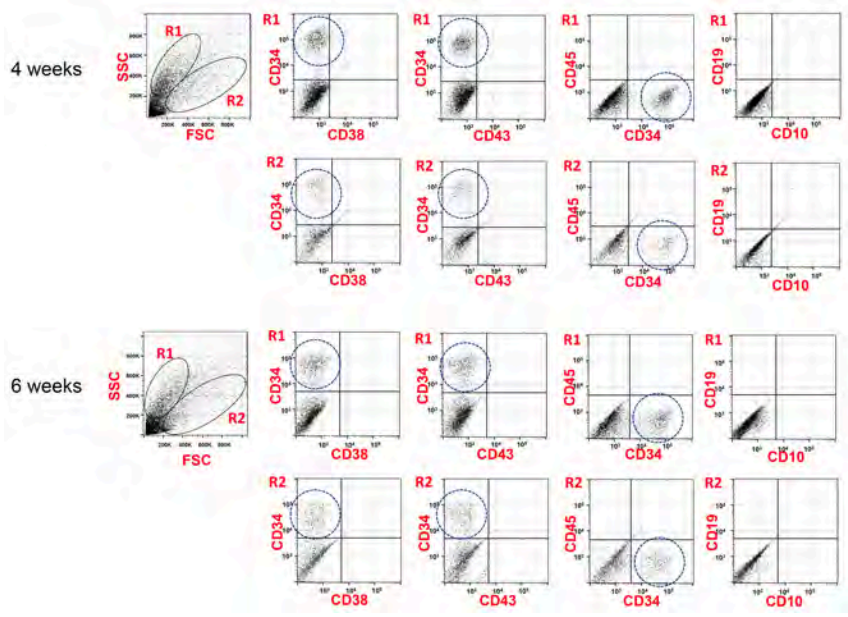


Figure S2

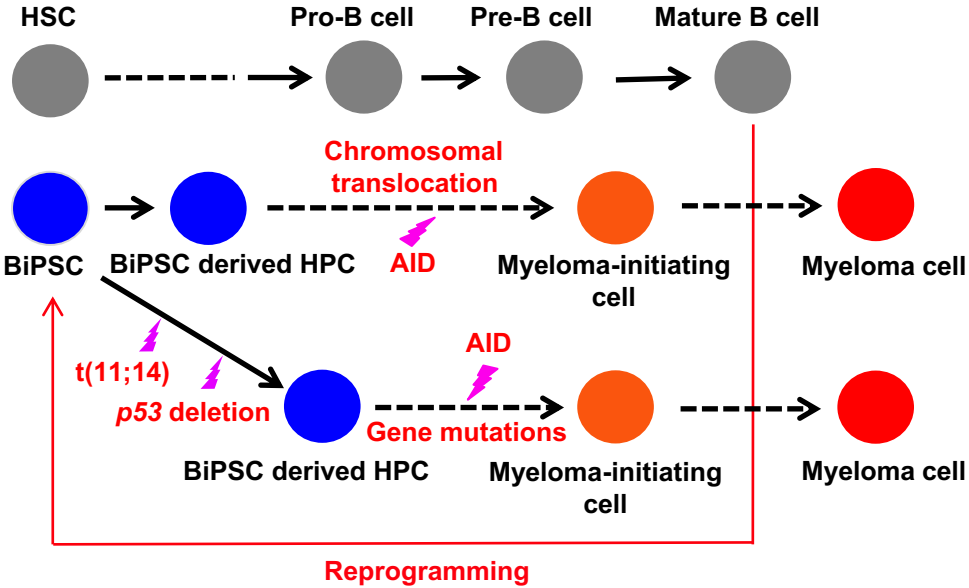
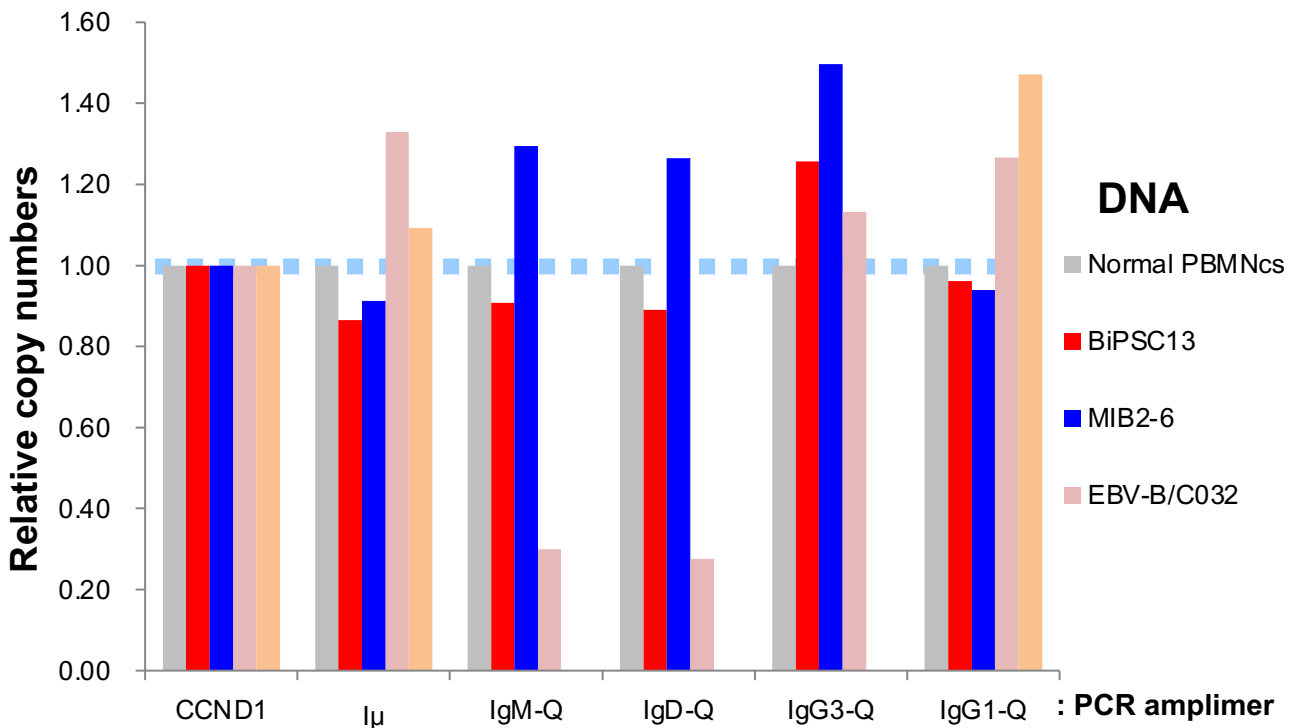


Figure S3



***IgH* gene**



Schematic Copy Number

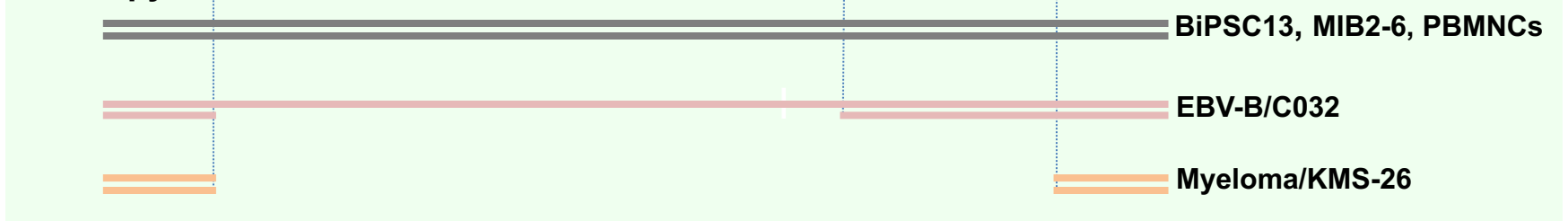


Figure S4

A

V3-9

<u>BiPSC13</u>	1	A A S G F T F D D Y A M H W V R Q A P G K G L E W V S G I S	90
<u>IGHV3-9*01</u>	66	TGCAGCCTCTGGATTACCTTTGATGATTATGCCATGCACTGGGTCCGGCAAGCTCCAGGGAAGGCCTGGAGTGGTCTCAGGTATTAG	155
		
		A A S G F T F D D Y A M H W V R Q A P G K G L E W V S G I S	

<u>BiPSC13</u>	91	W N S G S I G Y A D S V K G R F T I S R D N A K N S L Y L Q	180
<u>IGHV3-9*01</u>	156	TTGGAATAGTGGTAGCATAGGCTATGCGGACTCTGTGAAGGGCCGATTACCATCTCCAGAGACAACGCCAAGAAGTCCCTGTATCTGCA	245
		
		W N S G S I G Y A D S V K G R F T I S R D N A K N S L Y L Q	

D4-23

J2

<u>BiPSC13</u>	181	M N S L R A E D T A L Y Y C A K A V A H P Y W Y F D L W G R	270
<u>IGHV3-9*01</u>	246	AATGAACAGTCTGAGAGCTGAGGACACGGCCTTGATTACTGTGCAAAGGCGGTGGCCACCCTACTGGTACTTCGATCTCTGGGGCCG	293
		
		M N S L R A E D T A L Y Y C A	
<u>IGHD4-23*01</u>	7	-----	12
<u>IGHJ2*01</u>	1	-----	27

<u>BiPSC13</u>	271	G T L	279
<u>IGHJ2*01</u>	28	TGGCACCCCT	36
		

Figure S4

B

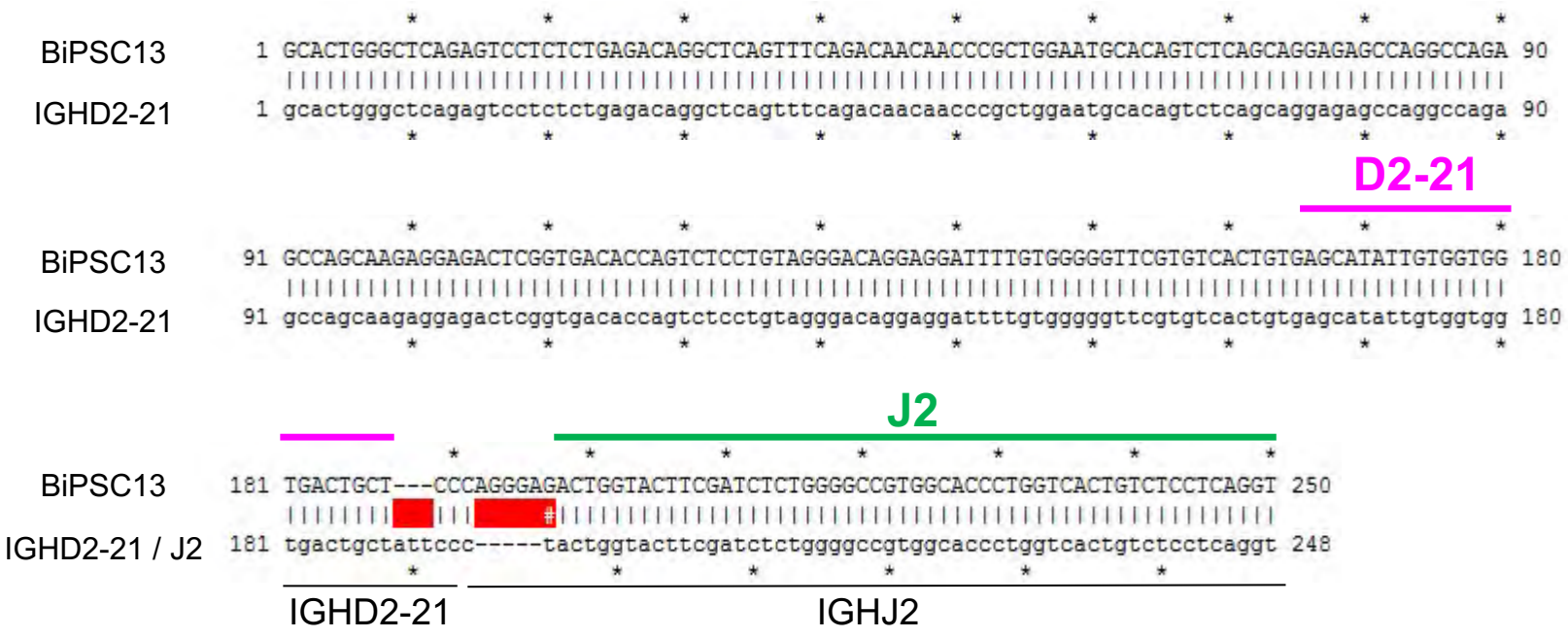


Figure S4

C

V4-39

MIB2-6	1	T V S G G S I S S S S Y Y W G W I R Q P P G K G L E W I G S	90
<u>IGHV4-39*07</u>	66	CACTGTCTCTGGTGGCTCCATCAGCAGTAGTAGTTACTACTGGGGCTGGATCCGCCAGCCCCAGGGAAGGGGCTGGAGTGGATTGGGAG	155
		
		T V S G G S I S S S S Y Y W G W I R Q P P G K G L E W I G S	

MIB2-6	91	I Y Y S G S T Y Y N P S L K S R V T I S V D T S K N Q F S L	180
<u>IGHV4-39*07</u>	156	TATCTATTATAGTGGGAGCACCTACTACAACCCGTCCTCAAGAGTCGAGTCACCATATCAGTAGACACGTCCAAGAACCAGTTCTCCCT	245
		
		I Y Y S G S T Y Y N P S L K S R V T I S V D T S K N Q F S L	

D3-22

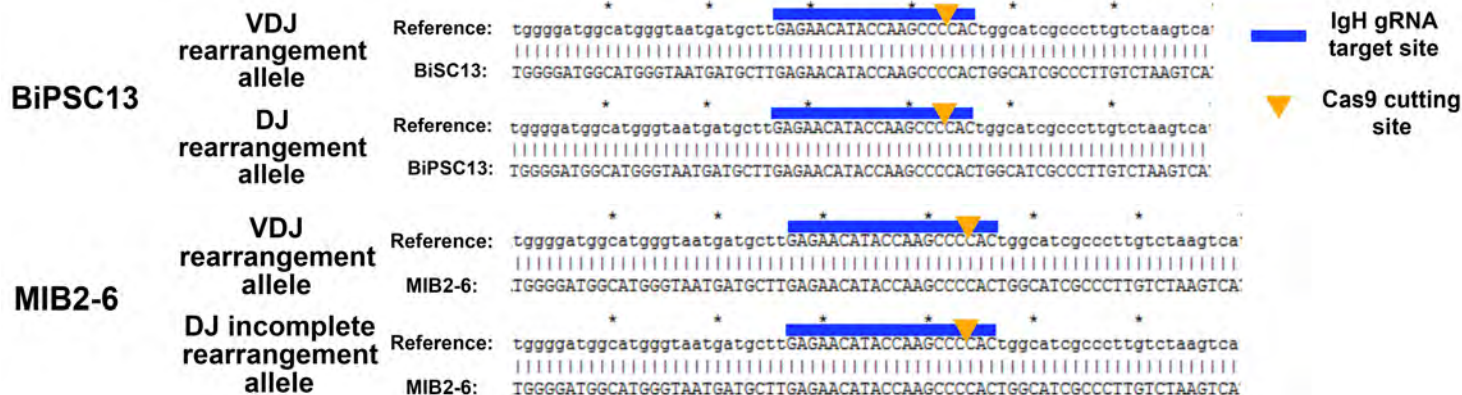
MIB2-6	181	K L S S V T A A D T A V Y Y C A R D V G G Y Y D S S G Y Y Q	270
<u>IGHV4-39*07</u>	246	GAAGCTGAGCTCTGTGACCGCCGCGACACGCGGTGATTACTGTGCGAGAGACGTAGGAGGTTACTATGATAGTAGTGGTTATTACCA	299
		
<u>IGHD3-22*01</u>	4	K L S S V T A A D T A V Y Y C A R	28

J6

MIB2-6	271	I Y Y Y Y Y G M D V W G Q G T T	318
<u>IGHJ6*02</u>	2	GATTTACTACTACTACTACGGTATGGACGTCTGGGGCCAAGGGACCAC	46

Figure S5

A



B

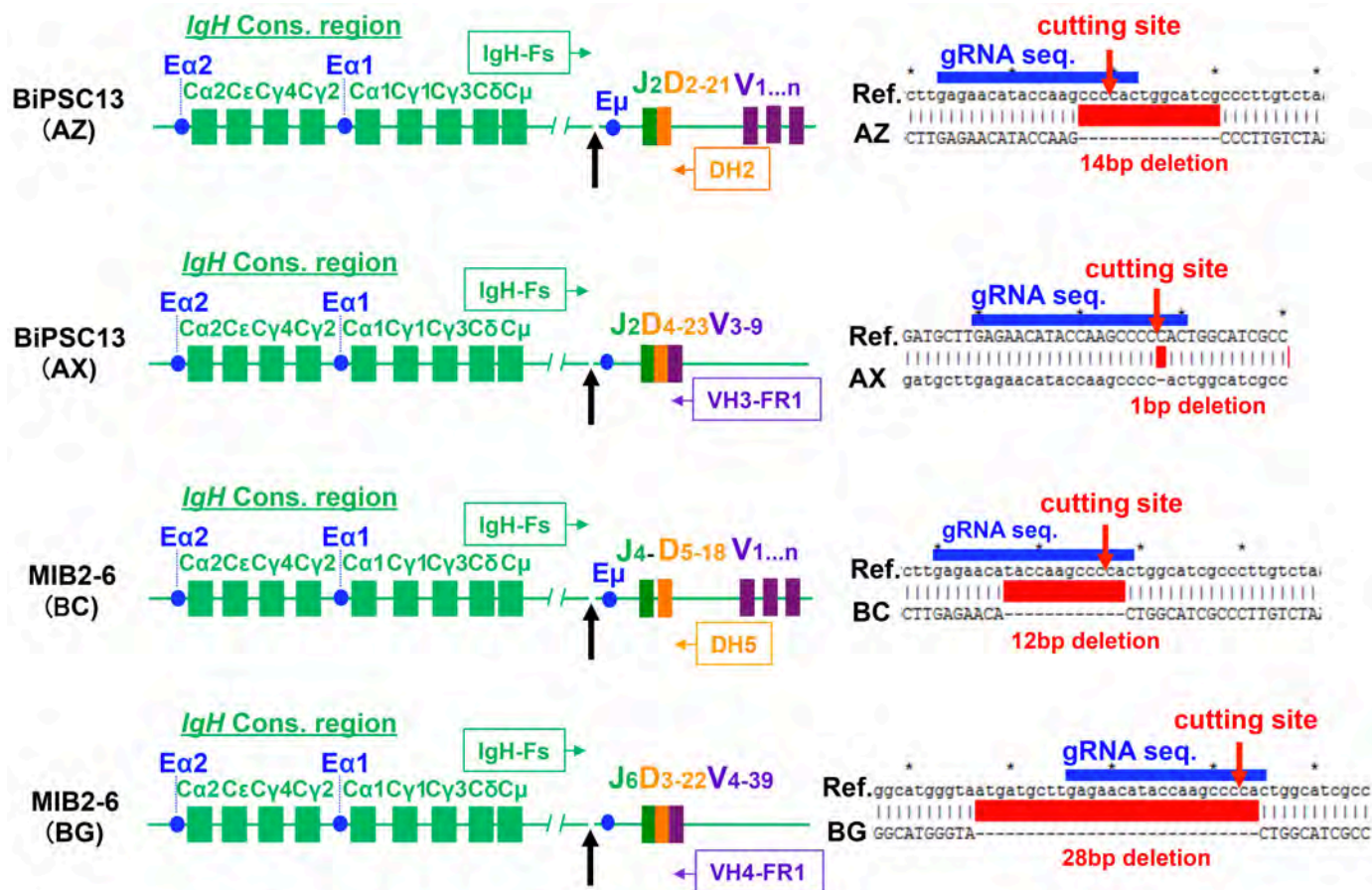
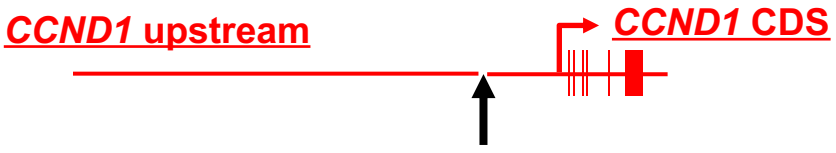


Figure S6

A

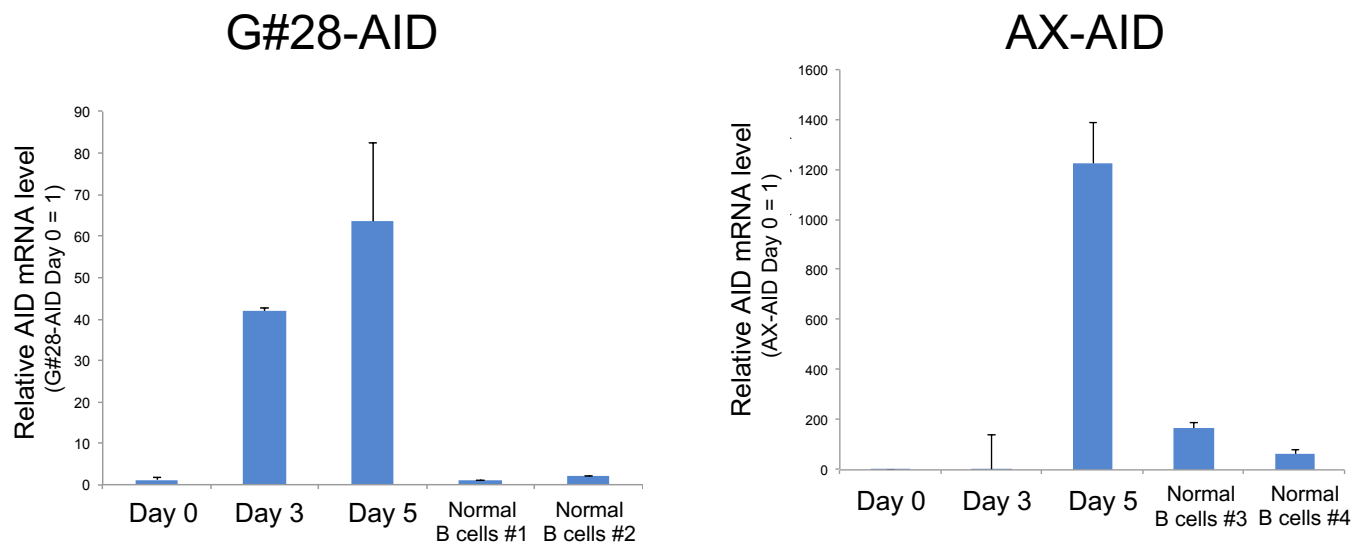


B

BiPSC13	Reference: cggctgtgcgagctggttgaatGTGGCGAGGTGGGACCGCGTggggctctgtgttgaaggtccagg BiPSC13: CGGCTGTGCGCAGCTGGTTGCAATGTGGCGAGGTGGGACCGCGTGGGGICTTGTGTTGAAGTCCAGG	<p>CCND1 gRNA target</p> <p>Cas9 cutting site</p>
BiPSC13 (AZ)	Reference: cggctgtgcgagctggttgaatGTGGCGAGGTGGGACCGCGTggggctctgtgttgaaggtccagg AZ: CGGCTGTGCGCAGCTGGTTGCAATGTGGCGAGGTGGG---11bp---GTCITGTGTTGAAGTCCAGG	
BiPSC13 (AX)	Reference: cggctgtgcgagctggttgaatGTGGCGAGGTGGGACCGCGTggggctctgtgttgaaggtccagg AX: CGGCTGTGCGCAGCTGGTTGCAATGTGGCGAGGTGGGAC---11bp---CTTGTGTTGAAGTCCAGG	
MIB2-6	Reference: cggctgtgcgagctggttgaatGTGGCGAGGTGGGACCGCGTggggctctgtgttgaaggtccagg MIB2-6: CGGCTGTGCGCAGCTGGTTGCAATGTGGCGAGGTGGGACCGCGTGGGGICTTGTGTTGAAGTCCAGG	
MIB2-6 (BG)	Reference: cggctgtgcgagctggttgaatGTGGCGAGGTGGGACCGCGTggggctctgtgttgaaggtccagg BG: CGGCTGTGCGCAGCTGGTTGCAATGTGGCGAGGTGGGACC---11bp---TTGTGTTGAAGTCCAGG	
MIB2-6 (BC)	Reference: ggtgctcgagttgggcatcttagcatgagaagctggaagtacatgatctcgggtgttttcatgacttctcagagctgcctttgcagacagacccctacc BC: GGTCICGAGT----- tcttggcactccaagcctgcttcaaatctcaagccagccgcctcttccaaagagaagccacgtgggatccctccctcctctgagctcctagagagcca 333bp ggatggcagtgaggaggaatgggtggtcacagactctggaggaagtcaactctccgtagagcaacacgtatggtgcctgagacacgtcggcaggtgtggg tggcggctgtgcgagctggttgaatGTGGCGAGGTGGGACCGCGTggggctctgtgttgaaggtccaggtccgtgcaacttgggggcaggggaccca ----- CGTGGGGICTTGTGTTGAAGTCCAGGTGCCGTGCACTTGGGGCAGGGCCACCA	

Figure S7

A



B

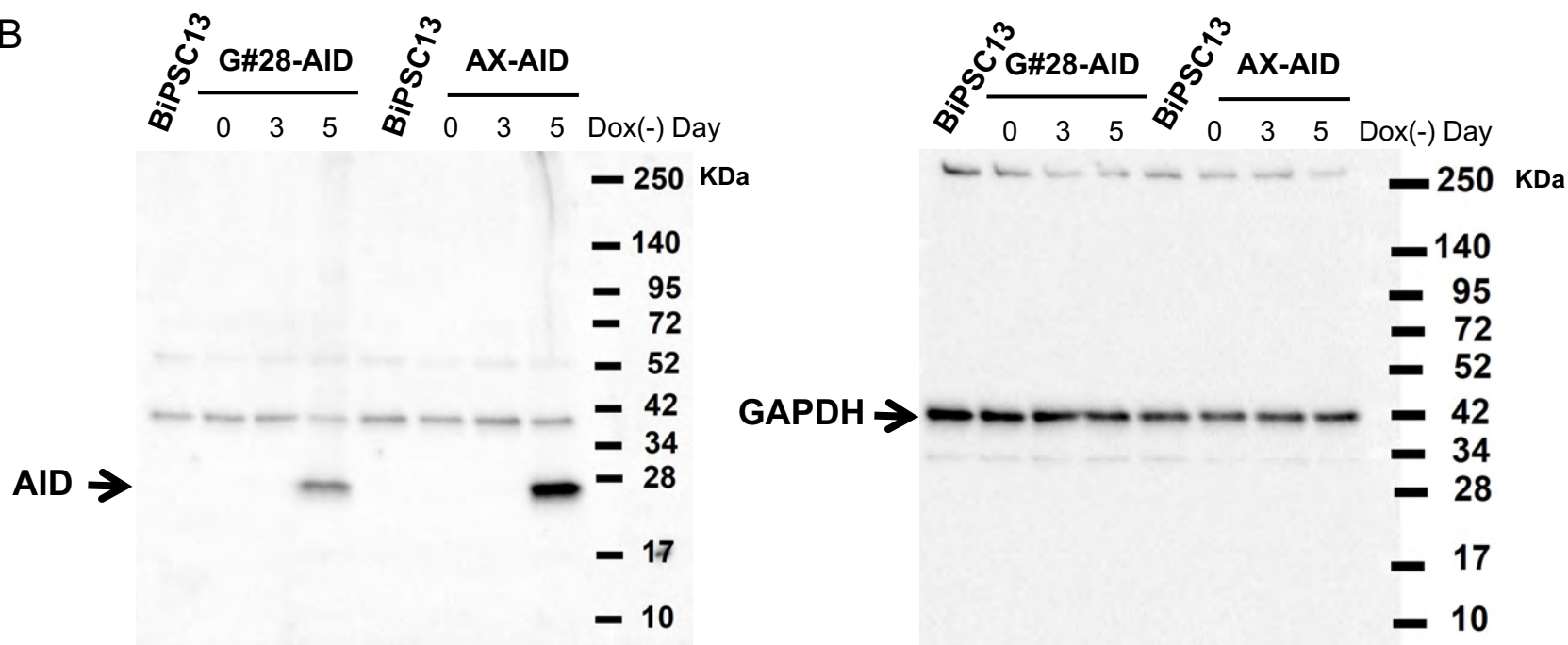
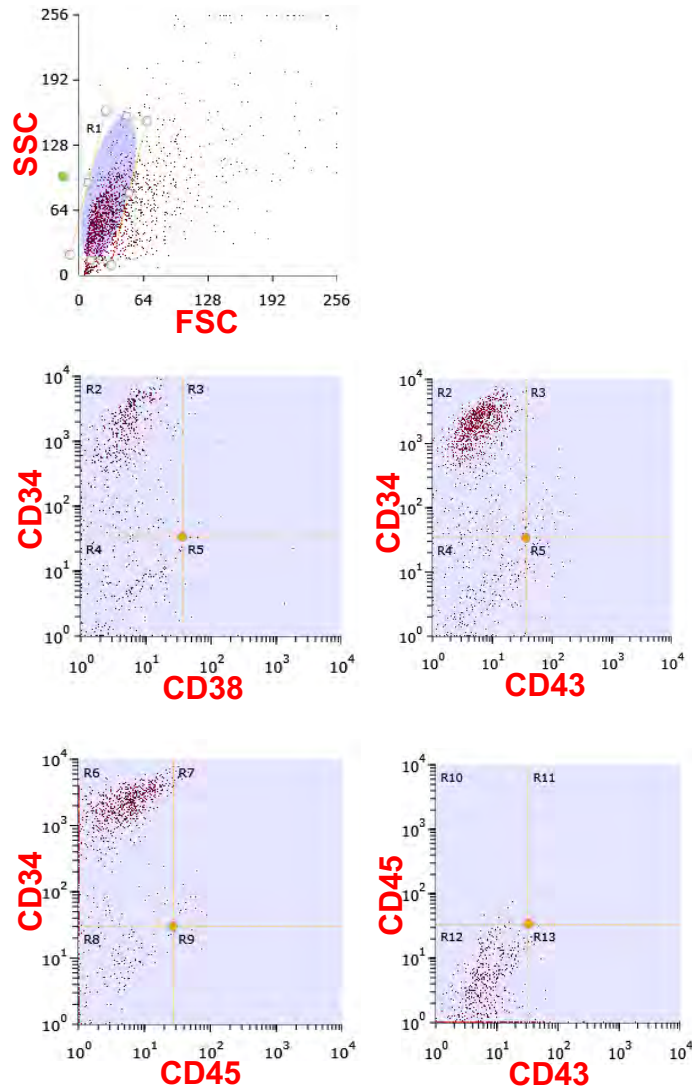


Figure S8

A



B

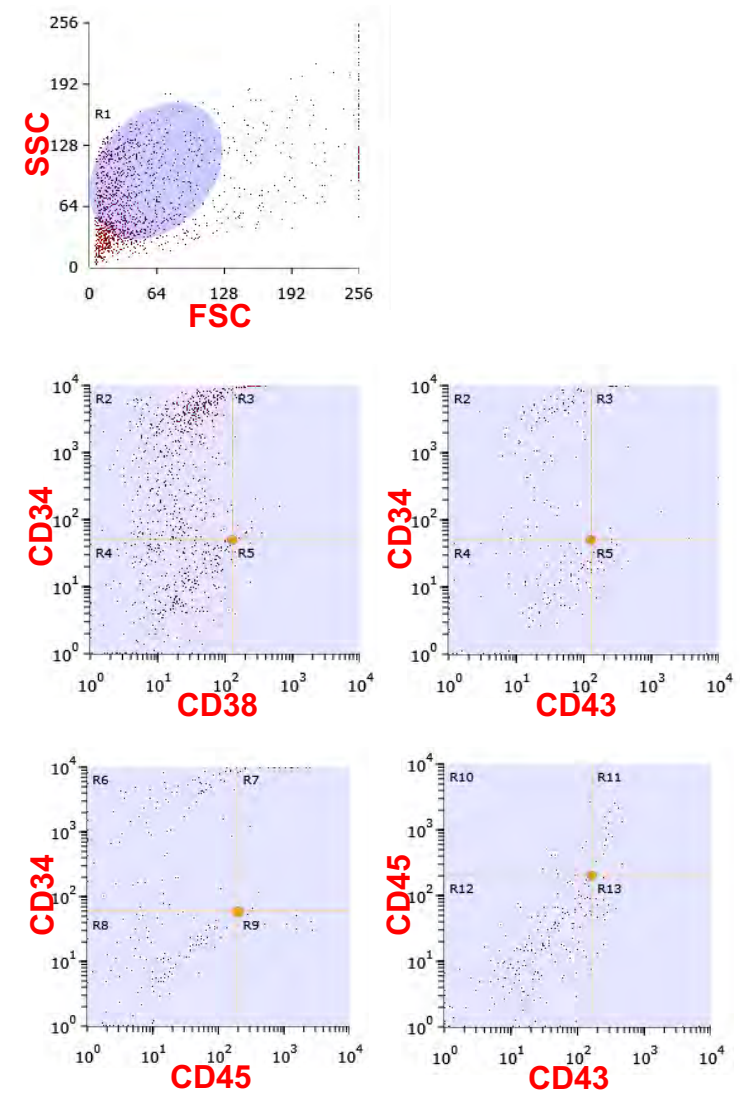
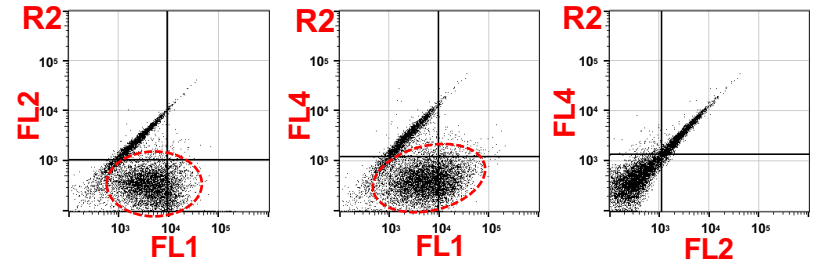
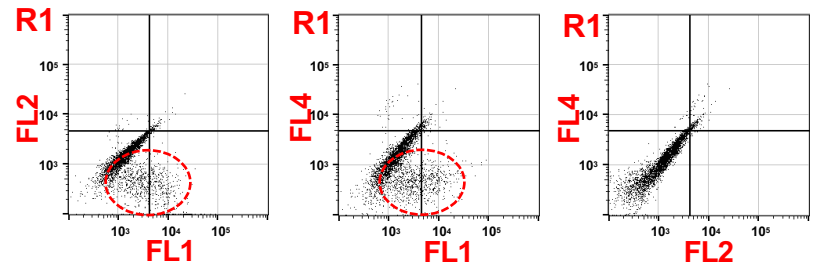
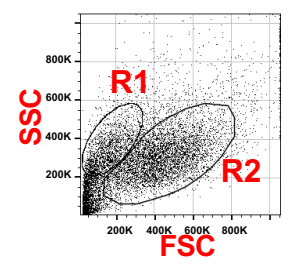


Figure S9

B BiPSC13/MS-5 (5W)

Non Stain



Isotype Control

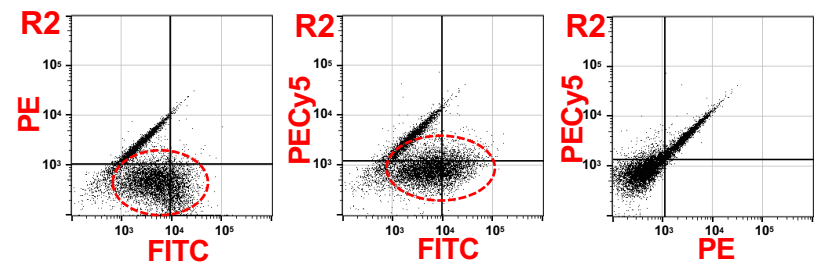
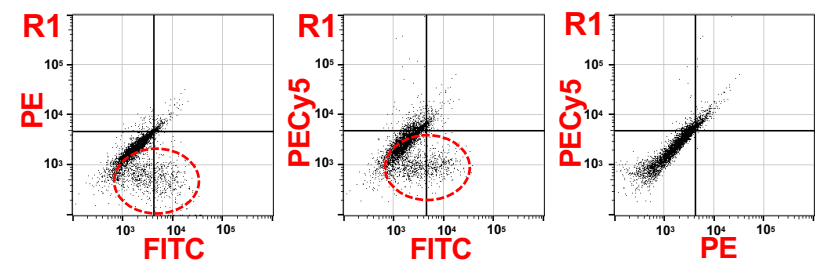
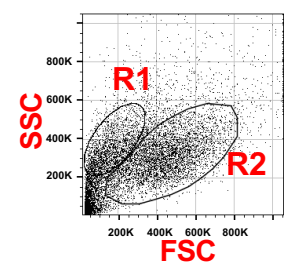


Figure S10

A NOP-2

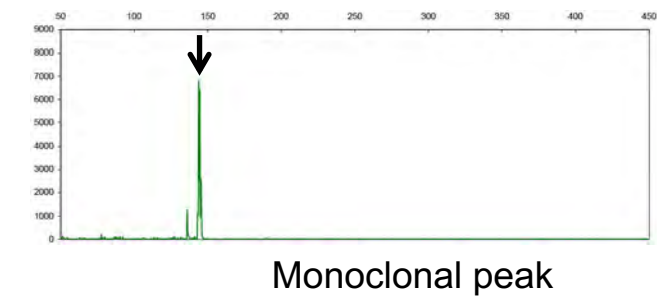
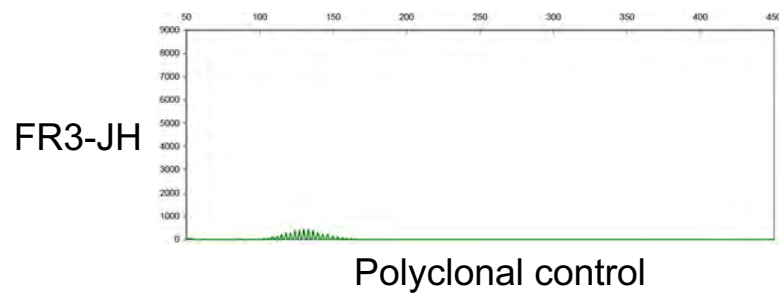
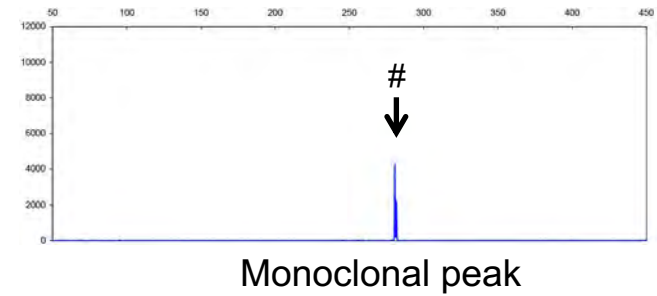
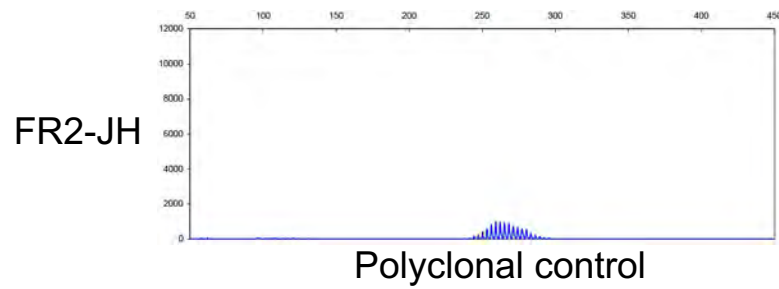
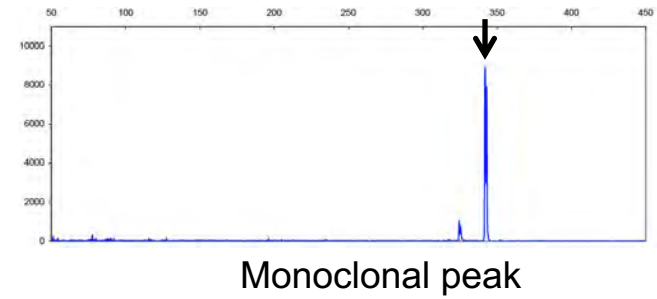
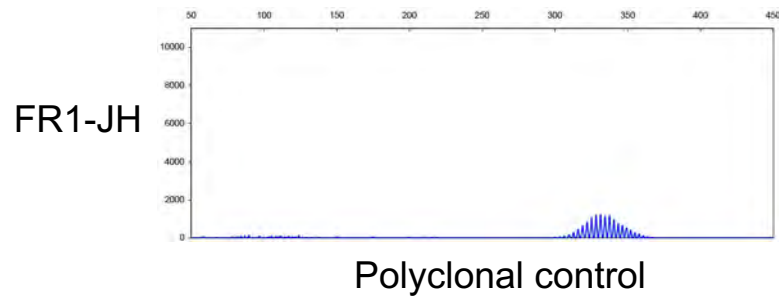


Figure S10

B

V1-46

NOP2 1 A S G Y **S** F T **D** Y **S** M H W V R Q A P G Q G L E W M G **V** **F** N P 90
IGHV1-46*01 70 GCATCTGGATACAGTTTCACCGACTACTCTATGCACTGGGTGCGACAGGCTCCTGGACAGGGGCTTGAGTGGATGGGAGTATTCAATCCG 159
CC.....AG.....A.....C.....A.....A.....A.....A.....C..T 159
 A S G Y T F T S Y Y M H W V R Q A P G Q G L E W M G I I N P

NOP2 91 S G **D** **V** T **T** Y A Q **T** F Q G R V **S** **I** **S** R D T **A** T S T V Y M E L 180
IGHV1-46*01 160 AGTGGTGATGTCACAACCTACGCGCAGACGTTTCAGGGCCGAGTCTCCATCTCCAGGGACACGGCCACGAGCACAGTCTATATGGAGCTG 249
G.AG.....G.....A.....A...C.....A.....A...GA.....T.....C..... 249
 S G G S T S Y A Q K F Q G R V T M T R D T S T S T V Y M E L

D5-18

NOP2 181 **R** S L R **A** E D T A **M** Y Y C A R D K W I **K** L W S T A P H Y **S** G 270
IGHV1-46*01 250 CGCAGCCTGAGAGCTGAGGACACGGCCATGTATTATTGTGCGAGAGATAAATGGATAAAGTTATGGTCCACAGCCCCCACTACTCCGGT 296
 A.....T.....G.....C.....
IGHD5-18*01 2 -----C..C..... 17
IGHJ6*02 10 -----A.... 20

J6

NOP2 271 M D V W G Q G T T 296
IGHJ6*02 21 ATGGACGTCTGGGGCCAAGGGACCAC 46

Figure S10

C

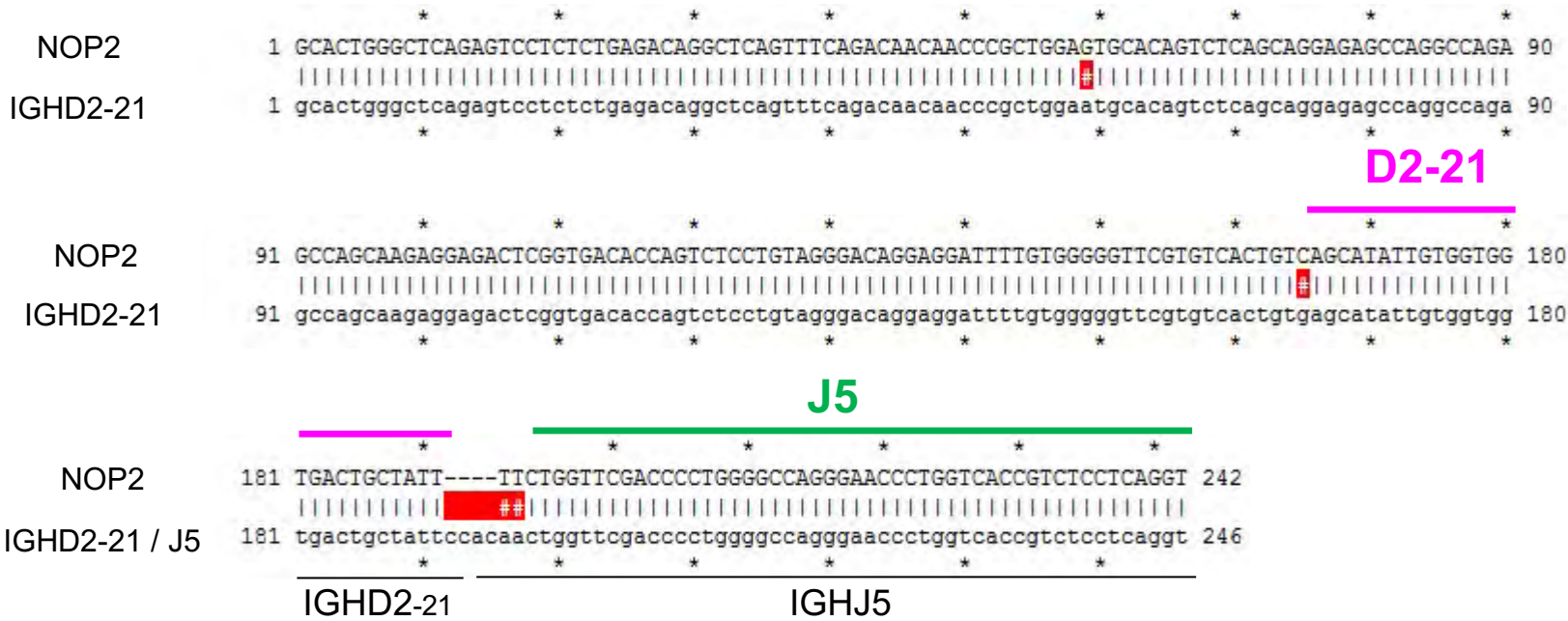


Figure S10

D KMS-12

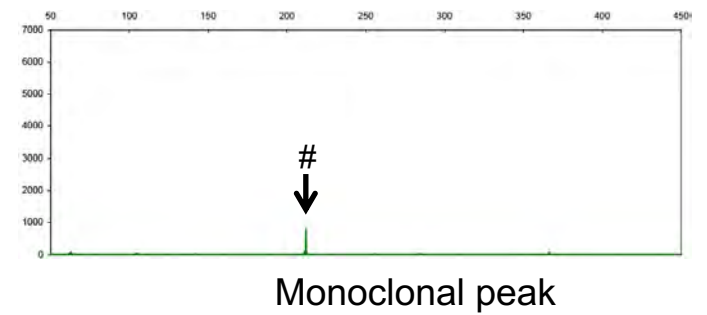
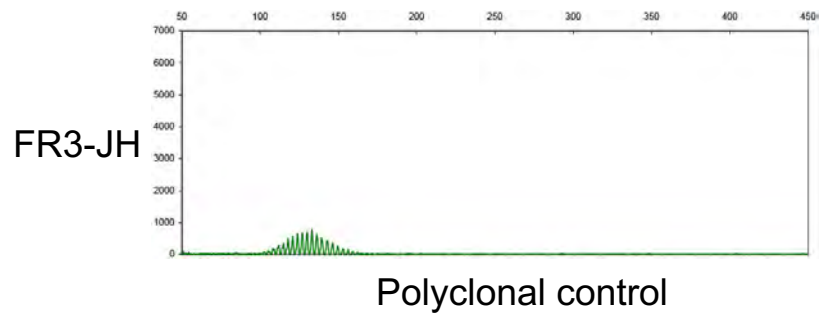
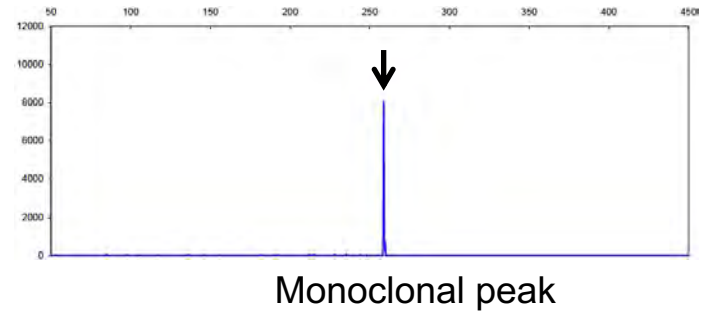
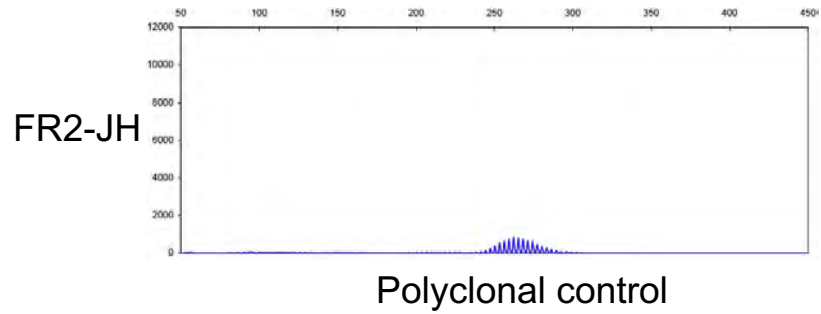
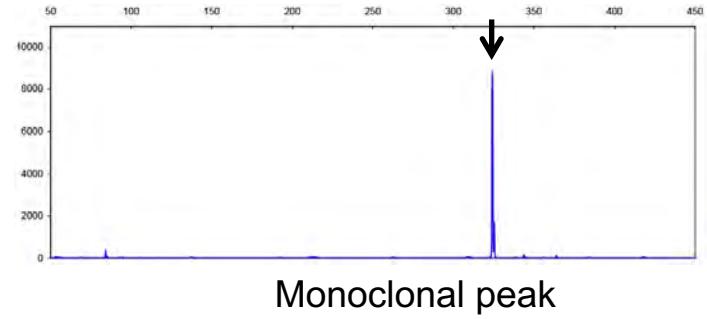
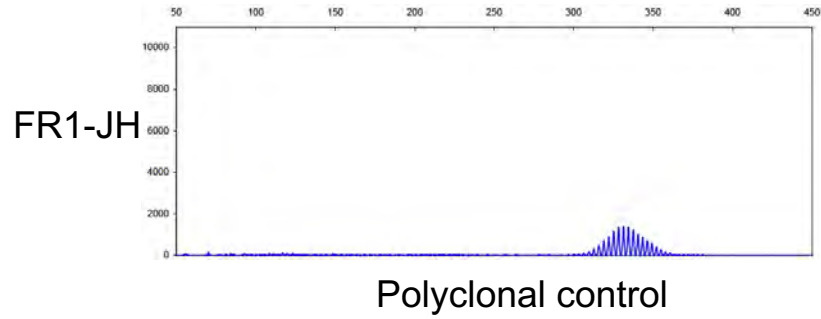


Figure S10

E

V3-7

KMS-12 1 A A S G F **S** F **G** **G** Y W M **N** W V R Q A P G K G L E W V A N **L** K 90
 IGHV3-7*01 66 TGCAGCCTCTGGATTTTCCTTTGGGGCTATTGGATGAATTGGGTCCGCCAGGCTCCAGGGAAGGGGCTGGAGTGGGTGGCCAATCTAAA 155
CA.....A.TA.....GC.....CA.....
 A A S G F **T** F **S** **S** Y W M **S** W V R Q A P G K G L E W V A N **I** K

KMS-12 91 **P** **G** **G** **G** **G** **D** **F** Y V D S V K G R F **I** I S **G** D N A K **K** S L **S** L Q 180
 IGHV3-7*01 156 ACCAGGGGGAGGTGGCGACTTCTATGTGGACTCGGTCAAGGGCCGATTCATCATCTCCGGAGACAACGCCAAGAAATCACTGTCCTTGCA 245
 G.A..AT...A...AGA.A.A.....T..G.....C.....A.....C.....A.C....
Q **D** **G** **S** **E** **K** **Y** Y V D S V K G R F **T** I S **R** D N A K **N** S L **Y** L Q

D4-23

J6

KMS-12 181 M N **R** L R **V** E D T A V Y Y C A R A G Y G G A G A M D V W G H 270
 IGHV3-7*01 246 AATGAACCGCTGAGAGTCGAAGACACGGCTGTCTATTACTGTGCGCGCCCGGATACGGTGGGGCAGGGGCTATGGACGTCTGGGGCCA 291
A.....C...G.....G.....
 M N **S** L R **A** E D T A V Y Y C A
 IGHV3-7*01 5 12
 IGHJ6*02 20 37

KMS-12 271 G T T 279
 IGHJ6*02 38 CGGGACCAC 46
 A.....

Table S1. Primers for PCR

<i>IgH</i> V region primers to confirm VDJ or DJ rearrangement	
VH1-FR1	GGCCTCAGTGAAGGTCTCCTGCAAG
VH2-FR1	GTCTGGTCCTACGCTGGTGAAACCC
VH3-FR1	CTGGGGGGTCCCTGAGACTCTCCTG
VH4-FR1	CTTCGGAGACCCTGTCCCTCACCTG
VH5-FR1	CGGGGAGTCTCTGAAGATCTCCTGT
VH6-FR1	TCGCAGACCCTCTCACTCACCTGTG
<i>IgH</i> D region primers to confirm VDJ or DJ rearrangement (5' to 3')	
DH1	GGCGGAATGTGTGCAGGC
DH2	GCACTGGGCTCAGAGTCCTCT
DH3	GTGGCCCTGGGAATATAAAA
DH4	AGATCCCCAGGACGCAGCA
DH5	CAGGGGGACACTGTGCATGT
DH6	TGACCCCAGCAAGGGAAGG
DH7	CACAGGCCCCCTACCAGC
<i>IgH</i> J primer to confirm VDJ or DJ rearrangement (5' to 3')	
JH consensus	CTTACCTGAGGAGACGGTGACC
Primers to confirm t(11;14)^{#1} (5' to 3')	
IgH-Fs ^{#2}	AAGGGTGCATGATGACCTAC
IgH μ -LoF ^{#3}	ATTTCCACTAGAAGGGGAAGTGGTCTTAAT
DH5-18-F	CCTACACCAGAGCCAGCAAAG
CCND1-86-F ^{#4}	CTTCTCACGAGCTGCCTTTG
CCND1-86-R	GCTCATCACACAGCTTGACG
CCND1-86-Rs	AGCTGTTCTTGTAGTGGTGCC
Primers to analyze copy number of <i>CCND1</i> and <i>IgH</i> constant region (5' to 3')	
CCND1-86-F	CTTCTCACGAGCTGCCTTTG
CCND1-86-Rt	GCCTACCACACCTCTTTTCCA
IgH-F	TTAGACAAGGGCGATGCCAG
IgH-R3	CCACTAGAAGGGGAAGTGGTC
IgM-Q-F	ACCGTGTCCGAAGAGGAATG
IgM-Q-R	TGGGTTTACCGGTGGACTTG
IgD-Q-F	GTACCACCCAACGTCCGTGA
IgD-Q-R	GATCTCCGGTGCACCTACC
IgG3-Q-F	GTCCCCACCTGACACTATCTTCTGT
IgG3-Q-R	AAGATCCACTTCACCTGTAGGCA
IgG1-Q-F	CCTGTATGAAACCCTGTCCCAC
IgG1-Q-R	CGGGTTTAGGTAAGAACAACGTG
Primers to clone AID open reading frame	
hAID-BamHI	TGGGATCCGCCACCATGGAC
hAID-EcoRI	CAGAATTCTCAAAGTCCCAAAGTAGG
Primers to analyze AID expression by qRT-PCR (5' to 3')	
AID-F	AAAATGTCCGCTGGGCTAAG
AID-R	AGGTCCCAGTCCGAGATGTAG

GAPDH-F	GGTGAAGGTCGGAGTCAACG
GAPDH-R	AATTTGCCATGGGTGGAATC

#1 Primers were positioned in translocation junction site.

#2 Primer for DNA sequence analysis of der(14)t(11;14)

#3 Primer for DNA sequence analysis of CRISPR/Cas9 target *IgH* site

#4 Primer for DNA sequence analysis of der(11)t(11;14)
and CRISPR/Cas9 target *CCND1* site